

Life Cycle Exposure to Environmentally Relevant Concentrations of Diphenyl Phosphate (DPhP) Inhibits Growth and Energy Metabolism of Zebrafish in a Sex-Specific Manner

Qiliang Chen,[○] Xiaolong Lian,[○] Jingjing An, Ningbo Geng,^{*} Haijun Zhang, Jonathan K. Challis, Yun Luo, Yaxin Liu, Guanyong Su, Yuwei Xie, Yingwen Li, Zhihao Liu, Yanjun Shen, John P. Giesy, and Yufeng Gong^{*}



Cite This: *Environ. Sci. Technol.* 2021, 55, 13122–13131



Read Online

ACCESS |



Metrics & More



Article Recommendations



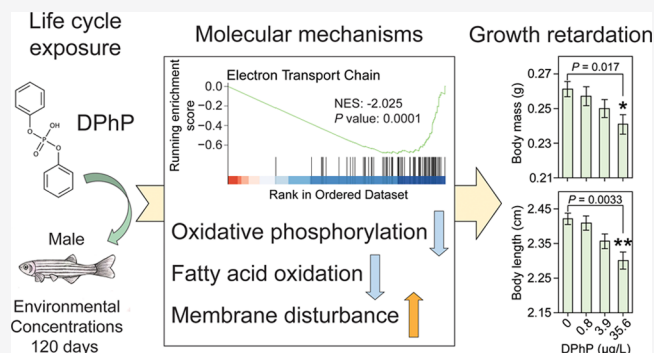
Supporting Information

ABSTRACT: Due to commercial uses and environmental degradation of aryl phosphate esters, diphenyl phosphate (DPhP) is frequently detected in environmental matrices and is thus of growing concern worldwide. However, information on potential adverse effects of chronic exposure to DPhP at environmentally realistic concentrations was lacking. Here, we investigated the effects of life cycle exposure to DPhP on zebrafish at environmentally relevant concentrations of 0.8, 3.9, or 35.6 $\mu\text{g/L}$ and employed a dual-omics approach (metabolomics and transcriptomics) to characterize potential modes of action. Exposure to DPhP at 35.6 $\mu\text{g/L}$ for 120 days resulted in significant reductions in body mass and length of male zebrafish, but did not cause those same effects to females. Predominant toxicological mechanisms, including inhibition of oxidative phosphorylation, down-regulation of fatty acid oxidation, and up-regulation of phosphatidylcholine degradation, were revealed by integrated dual-omics analysis and successfully linked to adverse outcomes. Activity of succinate dehydrogenase and protein content of carnitine *O*-palmitoyltransferase 1 were significantly decreased in livers of male fish exposed to DPhP, which further confirmed the proposed toxicological mechanisms. This study is the first to demonstrate that chronic, low-level exposure to DPhP can retard growth via inhibiting energy output in male zebrafish.

KEYWORDS: diphenyl phosphate, metabolomics, transcriptomics, gene set enrichment analysis (GSEA), oxidative phosphorylation, fatty acid oxidation

1. INTRODUCTION

Diphenyl phosphate (DPhP), an emerging environmental contaminant, is a major degradation product of several commonly used organophosphate (OP) flame retardants, such as triphenyl phosphate (TPhP),¹ resorcinol bis-(diphenylphosphate) (RDP),² and ethylhexyl diphenyl phosphate (EHDPHP).³ In addition, DPhP is being used directly as an industrial catalyst and additive.⁴ As a result of the diverse and heterogeneous sources mentioned above, DPhP has been detected to varying degrees, in a variety of media all over the world, such as human blood (<0.12–3.31 $\mu\text{g/L}$),⁵ human urine (0.14–32 $\mu\text{g/L}$,⁶ <0.16–193 $\mu\text{g/L}$,⁷ and 0.68–140 $\mu\text{g/L}$),⁸ indoor dust (923–79,661 ng/g),⁹ wastewater (0.03–1.29 $\mu\text{g/L}$),¹⁰ flowback and produced water (3.7 $\mu\text{g/L}$),¹¹ rivers (not detected–70 ng/L),¹² and wastewater sludge (0.93–1,680 ng/g dry weight).¹³ DPhP could be formed in fish by biotransformation of TPhP¹ and EHDPHP,^{14,15} which would contribute to the internal body burden of DPhP and further



highlights the importance of investigating toxicity of DPhP in fish.

Ubiquitous exposure to DPhP has raised concerns on risks to environment and human health.^{16,17} Results of previous studies have indicated that DPhP causes minimal acute toxicity. The 96 h-LC₅₀ value of DPhP to zebrafish embryos was 49.98 ± 7.06 mg/L.¹¹ DPhP caused no significant effects to chicken embryonic hepatocytes at concentrations up to 1000 μM (250 mg/L) but altered more transcripts than its precursor TPhP.¹⁸ In addition, exposure to DPhP could result in developmental toxicity, endocrine disruption, and cardiotoxicity.^{17,19–22} Recently, it was reported that chronic exposure to

Received: June 15, 2021

Published: September 15, 2021



10 mg/L DPhP through drinking water significantly disrupted the fatty acid catabolic processes and reduced the body mass in mice.²³ To date, most of the studies on toxicity of DPhP have only focused on acute toxicity/short-term effects upon exposure to DPhP at concentrations that are far greater than those found in environmental matrices, which are generally at in the range of $\mu\text{g/L}$.^{4,11,24} For example, DPhP-caused cardiac defects in zebrafish embryo were only observed at concentrations greater than 500 μM (125 mg/L).²¹ Exposure to DPhP increased mortality of zebrafish larvae but only at a concentration greater than 10^{-6} M (250 $\mu\text{g/L}$).²⁰ Currently, potential adverse effects of chronic exposure to DPhP at environmentally relevant concentrations is poorly characterized.

In addition, sex-dependent effects of exposure to TPhP, as well as other OP flame retardants, have been reported.^{25,26} For example, exposure to TPhP for 14 days significantly decreased concentrations of thyroxine and triiodothyronine in blood plasma of male zebrafish, whereas opposite effects were observed in females.²⁷ Exposure among pregnant women to relatively great concentrations of DPhP significantly increased risks of low birth weight for the newborns, and female newborns were more susceptible.¹⁶ However, it is still unknown if DPhP has sex-dependent effects on aquatic organisms.

Overall, the objective of this study was to determine effects of life cycle exposure to DPhP at environmentally realistic concentrations on zebrafish. Zebrafish embryos (2 h postfertilization) were exposed to DPhP at nominal concentrations of 0, 1, 10, or 100 $\mu\text{g/L}$ for 120 days until they reached sexual maturity. A dual-omics approach combining metabolomics and transcriptomics was applied. It was hypothesized that chronic exposure to environmentally relevant concentrations of DPhP would cause metabolomics and transcriptomic alterations of zebrafish, and such molecular responses would give novel insights into the modes of action of DPhP. This study is the first to comprehensively elucidate chronic toxicity of DPhP on aquatic organisms and of utmost importance for mechanism-based risk assessment of DPhP.

2. MATERIALS AND METHODS

2.1. Chemicals. DPhP (99% purity; CAS Registry Number: 838-85-7) was purchased from Shanghai Aladdin biochemical Technology Co., Ltd. Hendecanoic acid, nonadecanoic acid, L-phenylalanine-D⁵, (8,8,8-D³)-L-carnitine, 1,2-diheptadecanoyl-*sn*-glycero-3-phosphoethanolamine, and 1-lauroyl-2-hydroxy-*sn*-glycero-3-phosphocholine, purchased from Sigma (Shanghai, China) were used as internal standards for metabolome profiling. Methanol, water, and acetonitrile were of LC-MS grade from Fisher Scientific (Schwerte, Germany).

2.2. Zebrafish Breeding and Exposure. The current experiment was approved by the University of Saskatchewan (AUP# 20200065). Fertilized zebrafish embryos at 2 h post fertilization (hpf) were obtained from healthy adult fish (wildtype, AB strain) according to Zhang et al.²⁸ and were exposed to DPhP at nominal concentrations of 0, 1, 10, or 100 $\mu\text{g/L}$ for 120 days. There were four replicate tanks for each treatment and 150 embryos per tank. During the experimental period, fish were transferred to larger tanks as they grew to ensure that the experimental fish had enough living space. Half of the water in each aquarium was replaced every 2 days with fresh aerated tap water containing the desired concentration of

DPhP. Fish were fed thrice a day. Water temperature was maintained at 27 ± 0.3 °C with a 14/10 h light/dark controlled photoperiod. Dissolved oxygen and pH were >6 mg/L and 7.7 ± 0.1 , respectively. After a 120-day exposure, all fish were anesthetized with 0.01% MS-222 and dissected humanely after measurement of body length and body mass. Livers were excised and weighted to calculate the hepatosomatic index (HSI), determined as [liver mass (g)/body mass (g) \times 100%]. Then, all liver samples were flash-frozen in liquid nitrogen and stored at -80 °C for the analysis of metabolomics, transcriptomics, and enzyme activity. In this study, liver was selected for analysis for its central role in body energy metabolism and detoxification and metabolism of xenobiotic.²⁹ In addition, results of previous studies indicated that DPhP was most abundant in liver.²³ The sex of the fish was determined by visual inspection of gonadal morphology. The average sex ratio (proportion males) was 59.7%. More details for zebrafish maintenance and exposure design were provided in the [Supporting Information 1 \(SI\)](#).

2.3. Quantification of DPhP in Water. The actual exposure concentrations of DPhP in water from each exposure group were measured by use of a Waters Acquity Ultra Performance liquid chromatography system coupled online with an ABI Q-Trap 5500 (AB SCIEX, U.S.A.) mass spectrometer (UPLC-MS). Water samples in the middle layer of each tank were collected by use of plastic disposable droppers about 1 h after water renewal and stored at -80 °C until analysis. There were four replicates in each group. The limit of detection (LOD) of the method is 0.01 $\mu\text{g/L}$. See [SI 2](#) for more details.

2.4. Pseudotargeted Metabolomics. For pseudotargeted metabolomics analysis, eight zebrafish livers of the same sex randomly selected from the same exposure tank were pooled as one sample, and each treatment group had eight pooled samples. There were two pooled samples for each replicate tank and four replicate tanks for each treatment. Metabolites were extracted and analyzed based on previously published methods.^{30,31} Details of metabolite extraction and instrumental analysis are given in [SI 3](#). Metabolites were annotated by accurate mass and MS/MS matching to experimental spectra in the Human Metabolome Database (HMDB). Commercially available standards were further employed to validate these annotations during the method development stage. Peak picking and integration were performed with MultiQuant software (3.0.1, AB SCIEX) and manually checked to ensure data quality. For quantification, peak areas of each metabolite were normalized to corresponding internal standards after peak alignment and missing value interpolation. In addition, a quality control (QC) sample was prepared by pooling 10 μL of aliquots from each sample. QC samples were inserted after every six samples to monitor system stability during the run. Meanwhile, procedural blanks, consisting of extraction in the absence of actual sample, were conducted and analyzed to filter any contaminations introduced during sample preparation.

All metabolomics data were log-transformed to achieve normally distributed data before statistical analysis. Partial least-squares discriminate analysis (PLS-DA) was generated after autoscaling of the metabolomics data by MetaboAnalyst 5.0 online platform.³² Differential metabolites (DMs) were determined with the criteria of *P* value <0.05 and fold change >1.5 relative to control. Chemical similarity enrichment analysis (ChemRICH), which enables study-specific and background-independent enrichment analysis, was also per-

formed on the annotated metabolomics data set.³³ Chemical clusters with P adjusted <0.05 were considered significant. Cluster directions was determined by the median \log_2 fold change relative to control of DMs in each metabolite cluster.³⁴

2.5. Transcriptomic Profiling. Livers of zebrafish exposed to nominal concentrations of 0, 10, or 100 μg DPhP/L were used for transcriptomics. Each treatment group had three pooled samples and each pooled sample had eight zebrafish livers of the same sex. Total RNA was isolated by TRIzol reagent (Invitrogen) and the next-generation sequencing was performed on an Illumina HiSeq platform (SI 4). All raw reads were deposited into the NCBI Sequence Read Archive (SRA accession: PRJNA730648). Raw data was processed by Cutadapt software (v1.16; Table S1) and assembled genes were annotated for function against several public databases (Table S2). Transcript abundances were measured as fragments per kilobase of transcript sequence per millions base pairs sequenced (FPKM). Gene set enrichment analysis (GSEA) was performed using Wikipathways database by R package “clusterProfiler” to identify pathways disrupted by DPhP.³⁵ Gene expression were validated through quantitative real time PCR (qRT-PCR). Housekeeping elongation factor 1-alpha (*ef1a*) and ribosomal protein L13a (*rpl13a*) were employed as reference genes. Further qRT-PCR validation details are found in SI 5.

2.6. Protein Content and Enzyme Activity Assays. The protein contents of carnitine *O*-palmitoyltransferase 1 (CPT1) and activities of succinate dehydrogenase (SDH/respiratory complex II) and NADH-ubiquinone oxidoreductase (respiratory complex I) in zebrafish liver were determined by specific assay kits purchased from Nanjing Jiancheng Bioengineering Institute (Nanjing, China). The assays were performed according to the instructions of the manufacturer. All biochemical determinations were normalized to total protein content.

2.7. Statistics. All data are presented as mean \pm standard error (SE). Following testing for the normality assumption (Shapiro test) and variance homogeneity (Bartlett test), one-way analysis of variance followed by Tukey's HSD test (equal variances assumed) or Kruskal–Wallis test (equal variances not assumed) were employed to evaluate the significance of the mean differences. Differences were considered significant at $0.01 < P < 0.05$ and highly significant at $P < 0.01$. Hierarchical clustering analysis were produced by R package “Pheatmap”.³⁶

3. RESULTS AND DISCUSSION

3.1. Measured Exposure Concentrations. In this study, three time points were randomly selected during the 120-day exposure for measurement of DPhP in the exposure system. By UPLC–MS, mean concentrations of DPhP in water were $<$ LOD, 0.8 ± 0.2 , 3.9 ± 1.0 , and $35.6 \pm 9.9 \mu\text{g}/\text{L}$ corresponding to nominal exposure at 0, 1, 10, and 100 $\mu\text{g}/\text{L}$, respectively. Despite the deviations from the nominal, measured concentrations of DPhP in the life cycle exposure experiment were generally comparable among the three sampling points and exhibited narrow standard deviations (Table S3), which suggest that DPhP had reached stable equilibrium concentrations during the 120-day exposure.

To test the stability of DPhP, we exposed zebrafish embryos or adults to nominal 100 μg DPhP/L for 7 days and took water aliquots every 6 h for DPhP measurement. We found that aqueous concentrations of DPhP were quite stable during the 7-day exposure for zebrafish embryos (Figure S1). In contrast,

an obvious decline in the concentrations of DPhP in water was observed starting after approximately 4 days in the exposure for adult zebrafish (Figure S1). This data indicates that the differences between nominal and measured concentrations of DPhP might be due to microbial degradation and metabolism of DPhP by adult fish. Consistent with our results, previous studies have demonstrated that DPhP was resistant to pH-dependent hydrolysis³⁷ but can be degraded by glycerophosphodiester phosphodiesterase (GDPDs) which are widely expressed in prokaryotic and eukaryotic organisms.³⁸ Similar discrepancies between nominal and measured concentrations in the exposure water have also been reported previously for OP triesters, such as TPhP and EHDPHP.^{14,15,39,40} In comparison to TPhP and EHDPHP, the differences between nominal and measured concentrations of DPhP were relatively small in this study, which can be explained by greater chemical stability³⁷ and less bioconcentration potential of DPhP.^{4,41} Hereafter, all data were interpreted based on measured exposure concentrations of DPhP in water.

3.2. Effects of DPhP Exposure on Zebrafish Growth.

Life cycle exposure to 35.6 μg of DPhP/L for 120 days caused significant decreases in body mass and body length of male zebrafish, whereas no significant effects were observed for female zebrafish (Figure 1). A significant increase in HSI was also found in males after exposure to DPhP at 3.9 $\mu\text{g}/\text{L}$ when compared to the control group (Figure S2). No obvious effects on survival rate or condition factor were observed. DPhP has minimal acute toxicity and its 96h-LC₅₀ value was determined to be $49.98 \pm 7.06 \text{ mg}/\text{L}$ for zebrafish embryos.¹¹ Significantly

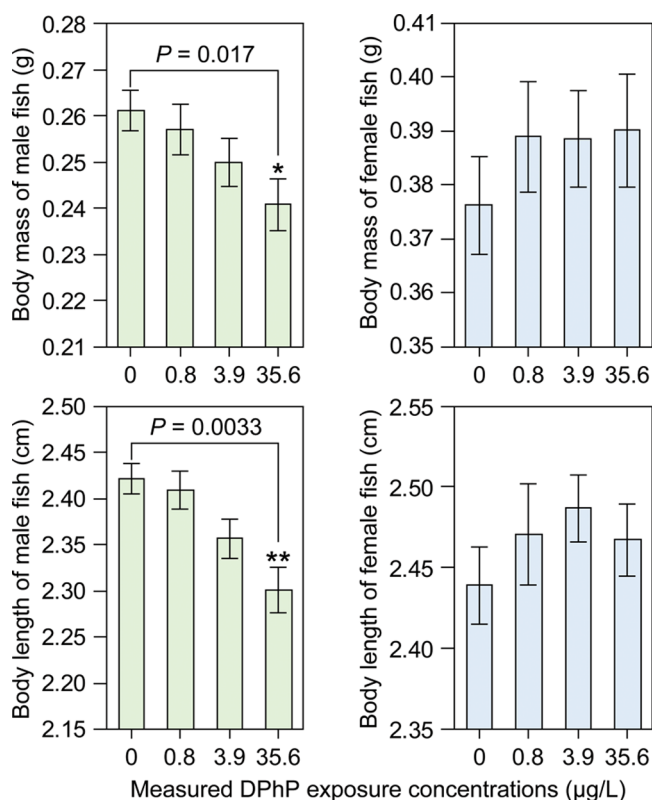


Figure 1. Effects of life cycle exposure to DPhP from fertilization to sexual maturity on body mass and length of zebrafish. Results are shown as the mean \pm SE ($N = 120$ fish per treatment group). The asterisk indicates significant differences between DPhP treatments and control ($*0.01 < P < 0.05$, $**P < 0.01$).

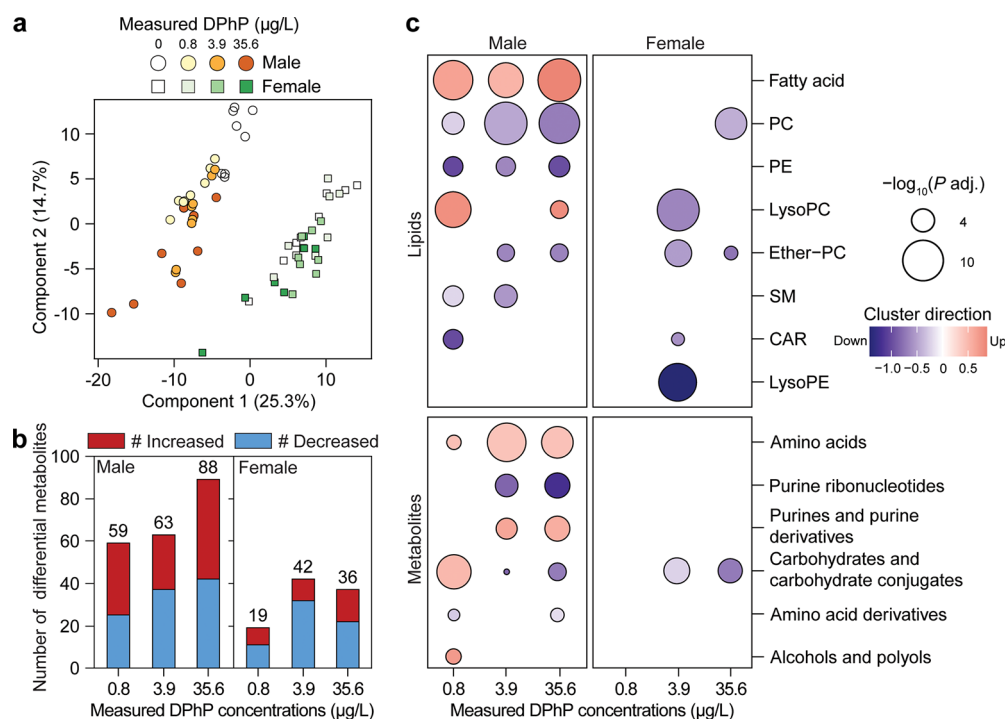


Figure 2. Changes in the metabolome of zebrafish liver after life cycle exposure to DPhP at environmentally realistic concentrations. (a) PLS-DA score plot. (b) Number of differential metabolites (DMs) in each exposure group. (c) Significantly enriched metabolite clusters identified by ChemRICH analysis. Pathway direction is the median \log_2 fold change of DMs relative to control in each cluster (blue, downregulated; red, upregulated). The dot size represents significance. PC: Phosphatidylcholine; PE: phosphatidylethanolamine; LysoPC: lysophosphatidylcholine; Ether-PC: Ether-linked phosphatidylcholine; SM: sphingomyelin; CAR: acylcarnitine.

greater mortality of embryos and lesser rates of hatching were observed in zebrafish after exposure to 10 μM (2.5 mg/L) DPhP from 4 to 96 hpf.²⁰ Recently, cardiotoxicity after acute exposure to high concentrations of DPhP (250 mg/L) have been observed, resulting in significantly greater distance between the sinus venosus and bulbus arteriosus (SV-BA) in zebrafish embryos.²¹ However, exposure to DPhP less than 30 μM (7.5 mg/L) did not induce circulatory failure in zebrafish embryos.²² These results imply that acute toxicity of DPhP was only present at extremely great concentrations. In the present study, we observed a sex-dependent effect of chronic exposure to DPhP at 35.6 $\mu\text{g/L}$ on male zebrafish growth. To our knowledge, this is the first study to demonstrate the chronic toxicity of exposure to DPhP at environmentally realistic concentrations.

3.3. Metabolomics Response. The metabolome includes intermediate and final products of cellular metabolism and can provide a direct “functional readout of the physiological state” of an organism in response to external stressors, which therefore make the metabolomics a valuable tool for mechanistic toxicology.^{42,43} The underlying relationship between growth and metabolites have been fairly characterized. For example, it has been demonstrated that lipids and fatty acids play major roles as sources of metabolic energy for fish growth.⁴⁴ Inhibition of mitochondrial fatty acid oxidation could reduce growth rate and feed utilization in fish.⁴⁵ To the knowledge of the authors, potential effects of DPhP on metabolome of any aquatic organisms have not been studied previously.

In the present study, we employed a pseudotargeted metabolomics approach to evaluate the chronic effects of exposure to DPhP at environmentally relevant concentrations

on zebrafish, and a total of 296 metabolites were accurately measured. 91.9% of detected metabolites showed relative standard deviation (RSD) less than 30% (Figure S3), demonstrating good method reproducibility. For male zebrafish, samples from treated groups were separated from the control group in the PLS-DA score plot (Figure 2a). Meanwhile, 59, 63, and 88 metabolites were identified as differential metabolites (DMs) in zebrafish exposed to 0.8, 3.9, or 35.6 μg of DPhP/L (Figure 2b). Together these results suggested exposure to DPhP at environmentally relevant concentrations disturbed normal metabolic processes in male zebrafish liver. However, for female fish, samples from different exposure groups appeared overlapped in the PLS-DA plot (Figure 2a), and only 19, 42, and 36 DMs were detected (Figure 2b). These results indicate that, compared to males, DPhP is less potent to disrupt cellular metabolism in female zebrafish liver. Detected metabolites were further subjected to ChemRICH analysis based on chemical similarity and ontology mapping.³³ In male fish liver, ChemRICH analysis showed that concentrations of fatty acids and amino acids were significantly greater, while phosphatidylcholines (PCs) and phosphatidylethanolamines (PEs) were significantly less in male fish liver after exposure to DPhP at all tested concentrations (Figure 2c). Differential regulations of purine metabolism and some other choline-containing phospholipids, like lysophosphatidylcholines (lysoPC), ether-linked phosphatidylcholines (ether-PC), and sphingomyelin (SM), were also observed in male fish liver after exposure. In contrast to male zebrafish, few classes of metabolites were significantly altered in livers of female zebrafish due to exposure to DPhP. The majority of altered metabolites were involved in metabolism of glycerophospholipids. This strong sex effect of DPhP exposure

on the hepatic metabolome is in line with our growth data, and further suggests that specific regulatory mechanisms in response to DPhP might exist between male and female zebrafish. Similar to results of the study presented here, neonatal exposure to TPhP or DPhP also led to sex-dependent metabolic disruptions in mice.⁴⁶ Although the effects of TPhP on the metabolome have been explored in several species, including mice,⁴⁷ zebrafish,⁴⁸ freshwater microalgae,⁴⁹ and earthworm,⁵⁰ alterations in metabolomics caused by DPhP had not been well-defined until recently and then only for mice.²³ Acylcarnitines and fatty acids were the most affected metabolites in liver of mice after oral exposure to DPhP.²³ Taken together with the current data, fatty acid metabolism and its related biological processes could be substantially disrupted by DPhP.

3.4. Transcriptomic Profiling and GSEA. In order to elucidate the underlying mechanisms of DPhP-induced growth retardation and metabolic disturbance, a transcriptomic analysis was conducted on zebrafish liver after exposure to DPhP. Because exposure to 3.9 or 35.6 μg of DPhP/L caused the most significant alterations of the metabolome of zebrafish, the current transcriptomic analysis solely focused on those two DPhP exposure groups. Pathway enrichment analysis performed by an advanced GSEA algorithm was employed to identify biological pathways that were affected by DPhP exposure. GSEA algorithm does not rely on arbitrary differentially expressed genes (DEGs) and can reduce potential bias and stringent limitations of conventional single gene differential expression analyses.⁵¹ In this study, GSEA analysis revealed significant inhibition of many pathways associated with energy metabolism in male fish liver after exposure to 3.9 or 35.6 μg of DPhP/L, including TCA cycle, oxidative phosphorylation, and electron transport chain (Figure 3 and

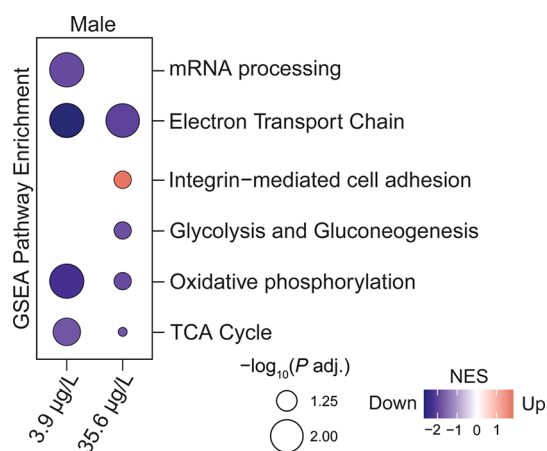


Figure 3. Wikipathways enrichment analysis of male zebrafish using gene set enrichment analysis (GSEA) algorithm. The dot size indicates pathway significance. The pathway direction is the normalized enrichment score (NES). Enriched pathways with P adjusted <0.1 were considered significant.

Table S4). Depressed glycolysis and gluconeogenesis and activated integrin-mediated cell adhesion were also observed in livers of male zebrafish exposed to 35.6 μg DPhP/L. Female zebrafish exhibited a distinct profile of gene expression when exposed to DPhP at 3.9 or 35.6 $\mu\text{g/L}$ (Figure S4). Significant enrichments of ERK1-ERK2/MAPK cascade, cytoplasmic ribosomal proteins, oxidative stress, transformation growth

factor beta receptor signaling pathway, and FGF signaling pathways were observed in female liver following chronic exposure to 3.9 $\mu\text{g/L}$ of DPhP. In response to exposure to 35.6 μg of DPhP/L, female zebrafish exhibited significant enrichment of cholesterol biosynthesis, exercise-induced circadian regulation, electron transport chain, oxidative phosphorylation, and FGF signaling pathway.

3.5. qRT-PCR Validation. Seven genes were selected randomly for validation of transcriptomic data. These genes included NADH: ubiquinone oxidoreductase subunit B4 (*ndufb4*), carnitine palmitoyltransferase 1B (*cpt1b*), carnitine palmitoyltransferase 1Ab (*cpt1ab*), pyruvate dehydrogenase kinase 2b (*pdk2b*), long chain acyl-CoA synthetase 4a (*acsl4a*), period circadian clock 1b (*per1b*), and nuclear receptor subfamily 1, group D, member 2b (*nrl2b*; Table S5). As shown in Table S6, the altered gene expression levels measured by qRT-PCR analysis were in accordance with that from RNA-seq, which independently verified our transcriptomic results.

3.6. Inhibition of Oxidative Phosphorylation. Four energy production-associated pathways, including electron transport chain, oxidative phosphorylation, glycolysis and gluconeogenesis, and TCA cycle, stood out at the top of the list ranked by P value as the most affected biological processes in male fish liver after exposure to 35.6 μg DPhP/L (Figure 4a). All four significantly enriched pathways have a negative normalized enrichment score (NES) value less than -1.5 , which is indicative of a strong down-regulation of these pathways and energy output in liver of male zebrafish. Consistent with the transcriptomic alterations, significant and dose-dependent decreases in ATP abundance were observed in male fish liver by pseudotargeted metabolomics (Figure 4b). It has been demonstrated that some environmental pollutants could hamper oxidative phosphorylation and ATP production by inhibiting electron transport complexes.^{52,53} Enzyme activity tests were conducted to see whether the altered transcriptomic pattern discussed above would lead to reduced electron transport chain activity and thereby ATP deficiency. Consistent with the omics data, a significant decrease in succinate dehydrogenase (SDH/respiratory complex II) enzyme activity was detected in male fish liver after exposure to 35.6 μg of DPhP/L (Figure 4c), while NADH-ubiquinone oxidoreductase (respiratory complex I) activity was not significantly altered (data not shown). Results of previous studies have shown that prolonged disruption of oxidative phosphorylation could contribute to lesser body mass.⁵⁴ In this study, for the first time, it was demonstrated that exposure to environmentally relevant concentrations of DPhP can result in inhibition of SDH enzyme, and through inhibition of oxidative phosphorylation, suppressed production of ATP, which could be the main cause of retardation of growth in male zebrafish.

3.7. Down-Regulated Fatty Acid Oxidation. In contrast to mammals who mainly use carbohydrates, fish prefer fatty acids as the metabolic energy source for growth.⁴⁴ Results of previous studies have suggested that impairment of fatty acid oxidation, caused by exposure to environmental pollutants, could lead to reduced growth of individual fish.^{45,55,56} For example, down-regulation of fatty acid oxidation and dysfunction of mitochondria were observed in zebrafish exposed to tris(1,3-dichloro-2-propyl) phosphate (TDCIPP), which resulted in suppression of ATP synthesis and further affected the growth and development of zebrafish.⁵⁷ As shown in Figure 5a, exposure to DPhP significantly increased the total abundance of free fatty acids in male fish

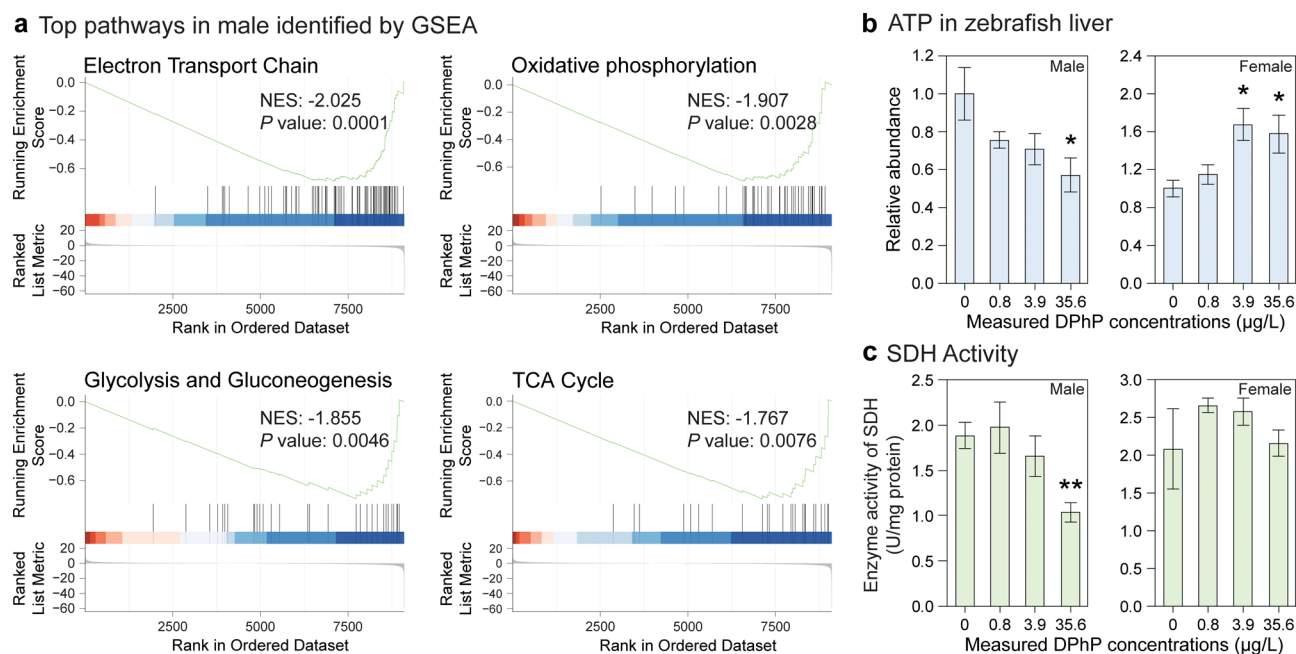


Figure 4. Inhibition of energy output in male zebrafish liver after life exposure to DPhP at environmentally realistic concentrations. (a) Gene set enrichment analysis (GSEA) results showing negative regulation of the energy metabolism related pathways in male fish liver after exposure to 35.6 $\mu\text{g/L}$ of DPhP. The colored bars indicate the fold change in gene expression (red; up-regulated; blue: down-regulated). NES: normalized enrichment score. (b) Altered relative abundance of ATP in zebrafish liver by DPhP exposure. $N = 8$. (c) Enzyme activity of succinate dehydrogenase (SDH) in zebrafish liver. $N = 4$. The asterisk indicates significant differences between DPhP treatments and control ($*0.01 < P < 0.05$, $**P < 0.01$).

liver, while no significant effects were observed in female. A closer examination of fatty acid profile revealed that a total of 11 long-chain and very long-chain fatty acids were significantly increased (Figure 5b). In order to oxidize fatty acids for energy in the mitochondria, free fatty acids in the cytoplasm must first be activated to acyl-CoA, a process that is modulated by acyl-CoA synthetases, and then transported into mitochondrial matrix through the carnitine shuttle system.⁵⁸ Carnitine shuttle system is comprised of two carnitine palmitoyltransferases (CPTs), CPT1, and CPT2. CPT1 catalyzes the transesterification of acyl-CoA to acyl-carnitine which is the rate-limiting step of the fatty acid oxidation.⁵⁹ Consistent with the pseudotargeted metabolomics data, it was found that expressions of genes encoding acyl-CoA synthetases (*acs14a* and *acs14b*) and CPT1 isoforms (*cpt1ab* and *cpt1b*) were decreased in a dose-dependent manner in male zebrafish exposed to DPhP (Figure 5c). We further determined the protein content of CPT1 enzyme in male fish liver and as expected, a significant decrease was observed in 35.6 μg DPhP/L exposure group (Figure 5d). These results clearly indicate that life cycle exposure to DPhP at environmentally realistic concentrations caused deficiency of fatty acid oxidation in male fish liver via inhibition of fatty acid activation and transport across mitochondrial membrane. Down-regulated catabolism of fatty acid would further contribute to the growth retardation of male zebrafish (Figure 1). Similarly, a clear reduction of fatty acid catabolic processes by DPhP exposure was also demonstrated in mice liver.²³ Results presented here were consistent with previous findings but also further revealed the key steps in fatty acid oxidation pathway that was specifically disrupted by DPhP.

3.8. Membrane Disturbance. PC is the major constituent of the eukaryotic membrane and represents 40% of phospholipids in most cellular membranes.⁶⁰ In the present

study, significantly decreased total PC abundances were observed in liver of male zebrafish after exposure to 3.9 or 35.6 μg of DPhP/L for 120 days, while abundances of its metabolic products, such as lysoPC, glycerophosphocholine, and choline, were all significantly increased after exposure to 35.6 μg of DPhP/L (Figure S6). This result suggested an upregulated catabolism of PC molecules and the subsequent release of choline. In addition, it has been demonstrated that exposure to lysoPC could increase intracellular mitochondrial permeability and disrupt mitochondrial integrity and function, thereby decreasing fatty acid oxidation and energy production.⁶¹ Taken together, breakdown of PCs and increased lysoPC abundance observed in this study might indicate potential damage to the mitochondrial membrane, which could contribute to depressed energy metabolism in male zebrafish liver after life cycle exposure to DPhP. Specific tests for mitochondrial membrane integrity are required to confirm the hypothesis in the future. By using RNA-seq, Mitchell et al.²¹ reported that acute exposure to 500 μM of DPhP significantly altered pathways associated with mitochondrial dysfunction and mitochondrial-specific structures and processes in zebrafish embryo at 30 hpf, which supports our assumption.

3.9. Proposed Molecular Mechanisms of DPhP. Generally, the presence of DPhP in aquatic systems and human samples was at $\mu\text{g/L}$ levels.⁴ Previous toxicity studies on DPhP have employed extremely high exposure concentrations (mg/L levels) to invoke significant biological responses over acute or short-term exposures. These studies provide important information on the toxicology of DPhP, but realistic exposure scenarios in aquatic ecosystems will mostly be long-term exposures to low concentrations. In this study, the DPhP exposure concentrations used are comparable to those detected in DPhP-contaminated water bodies and in human urine samples. Our data, for the first time,

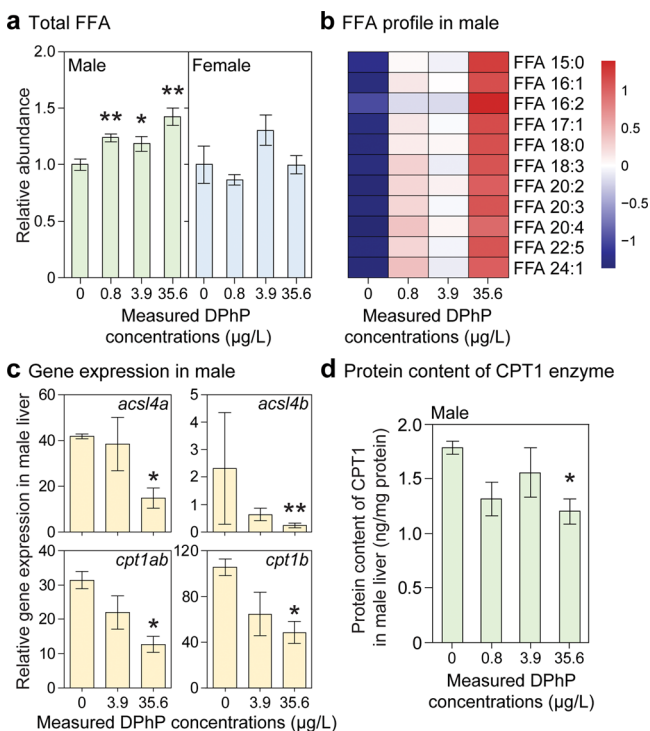


Figure 5. Effects of life cycle exposure to DPhP at environmentally realistic concentrations on fatty acid oxidation in zebrafish liver. (a) Total free fatty acid (FFA) abundance. (b) FFA profiles in male fish liver. Data were log-transformed and Z-scaled for heatmap plot. (c) Altered expression levels of genes related to fatty acid oxidation in male zebrafish liver. *acsl4a*: acyl-CoA synthetase long-chain family member 4a; *acsl4b*: acyl-CoA synthetase long chain family member 4b; *cpt1ab*: carnitine palmitoyltransferase 1Ab; *cpt1b*: carnitine palmitoyltransferase 1B. (d) Altered protein content of CPT1 enzyme in male zebrafish liver after exposure to DPhP. The asterisk indicates significant differences between DPhP treatments and control (*0.01 < P < 0.05, **P < 0.01).

demonstrated that life cycle exposure to environmental dose-related DPhP inhibits growth of male zebrafish. Through integration of metabolomics and transcriptomics, we proposed three possible mechanisms of DPhP toxicity (Figure 6), which were also confirmed at the protein or enzyme activity levels. First, exposure to DPhP decreases enzyme activity of SDH (respiratory complex II), and thereby reduces oxidative phosphorylation process in male zebrafish liver. Second, DPhP could also reduce expression of CPT1 protein which leads to the inhibition of fatty acid transport and oxidation. Finally, integrity of mitochondrial membrane might be decreased because of the accelerated degradation of PC molecules. These mechanisms should jointly contribute to the decreased energy output in male zebrafish and eventually lead to growth retardation. Based on data obtained, we deduced that mitochondria could be a main target for DPhP induced toxicity. Our study shed light on the molecular mechanisms of DPhP and implied important risks of DPhP to aquatic organisms. Retardation of growth caused by exposure to DPhP might have adverse effects on maintenance of fish populations, because animal body size is involved in many aspects of physiology and ecological performance, such as foraging, reproductive success, and longevity.^{62–64} In the future, it would be interesting to investigate the impacts of life-cycle exposure to DPhP on reproduction or swimming behavior of zebrafish, due to the deep correlation between energy metabolism and those biological processes. In addition, our findings may suggest a potential threat of DPhP to human health, in view of the fact that the sequence of mitochondrial DNA and nuclear mitochondrial proteins are relatively conservative between zebrafish and humans.⁶⁵ However, additional cautious apply when translating conclusions to human conditions when considering that the exposure routes may not be equivalent to the experience of human populations.⁶⁶

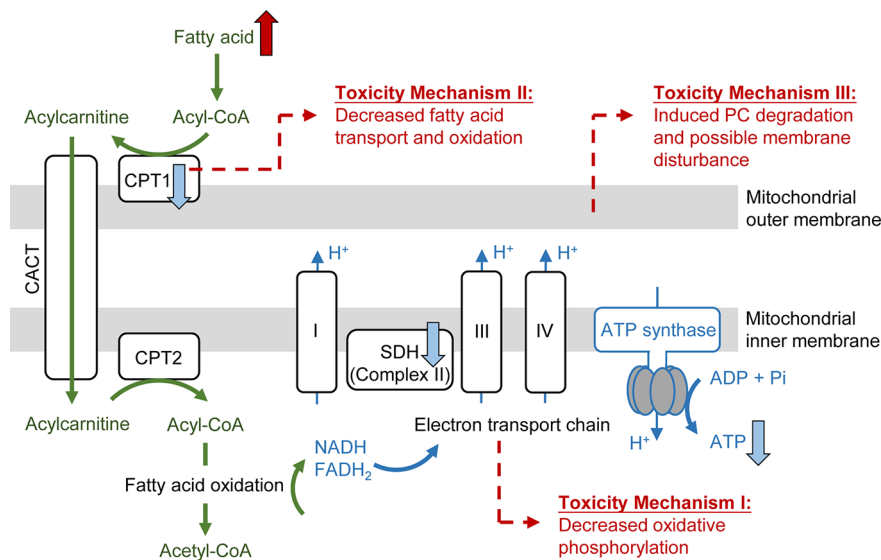


Figure 6. Proposed toxicity mechanisms of life cycle exposure to DPhP at environmentally relevant concentrations. CPT1: carnitine O-palmitoyltransferase 1; CPT2: carnitine palmitoyltransferase 2; CACT: carnitine-acylcarnitine translocase; SDH: succinate dehydrogenase/respiratory complex II.

■ ASSOCIATED CONTENT

Supporting Information

The Supporting Information is available free of charge at <https://pubs.acs.org/doi/10.1021/acs.est.1c03948>.

Detailed description on zebrafish maintenance, quantification of DPHP in water, sample preparation and instrumental analysis for pseudotargeted metabolomics, RNA isolation and sequencing, quantitative real time PCR (qRT-PCR), and a number of supporting tables and figures (PDF)

■ AUTHOR INFORMATION

Corresponding Authors

Ningbo Geng – CAS Key Laboratory of Separation Sciences for Analytical Chemistry, Dalian Institute of Chemical Physics, Chinese Academy of Sciences, Dalian 116023 Liaoning, China; Email: gengningbo@dicp.ac.cn

Yufeng Gong – Toxicology Centre, University of Saskatchewan, Saskatoon S7N 5B3 SK, Canada; orcid.org/0000-0002-1396-527X; Email: yufeng.gong@usask.ca

Authors

Qiliang Chen – Chongqing Key Laboratory of Animal Biology, School of Life Sciences, Chongqing Normal University, Chongqing 401331, China

Xiaolong Lian – Chongqing Key Laboratory of Animal Biology, School of Life Sciences, Chongqing Normal University, Chongqing 401331, China

Jingjing An – Chongqing Key Laboratory of Animal Biology, School of Life Sciences, Chongqing Normal University, Chongqing 401331, China

Haijun Zhang – CAS Key Laboratory of Separation Sciences for Analytical Chemistry, Dalian Institute of Chemical Physics, Chinese Academy of Sciences, Dalian 116023 Liaoning, China; orcid.org/0000-0001-5567-7834

Jonathan K. Challis – Toxicology Centre, University of Saskatchewan, Saskatoon S7N 5B3 SK, Canada; orcid.org/0000-0003-3514-0647

Yun Luo – CAS Key Laboratory of Separation Sciences for Analytical Chemistry, Dalian Institute of Chemical Physics, Chinese Academy of Sciences, Dalian 116023 Liaoning, China

Yaxin Liu – School of Environmental and Biological Engineering, Nanjing University of Science and Technology, Nanjing 210094 Jiangsu, China

Guanyong Su – School of Environmental and Biological Engineering, Nanjing University of Science and Technology, Nanjing 210094 Jiangsu, China; orcid.org/0000-0003-4356-5194

Yuwei Xie – Toxicology Centre, University of Saskatchewan, Saskatoon S7N 5B3 SK, Canada; orcid.org/0000-0001-5652-6413

Yingwen Li – Chongqing Key Laboratory of Animal Biology, School of Life Sciences, Chongqing Normal University, Chongqing 401331, China

Zhihao Liu – Chongqing Key Laboratory of Animal Biology, School of Life Sciences, Chongqing Normal University, Chongqing 401331, China

Yanjun Shen – Chongqing Key Laboratory of Animal Biology, School of Life Sciences, Chongqing Normal University, Chongqing 401331, China

John P. Giesy – Toxicology Centre, University of Saskatchewan, Saskatoon S7N 5B3 SK, Canada; Department of Veterinary Biomedical Sciences, University of Saskatchewan, Saskatoon S7N 5B4 SK, Canada; Department of Environmental Sciences, Baylor University, Waco, Texas 76798-7266, United States; State Key Laboratory of Pollution Control and Resource Reuse, School of the Environment, Nanjing University, Nanjing 210023 Jiangsu, China

Complete contact information is available at: <https://pubs.acs.org/doi/10.1021/acs.est.1c03948>

Author Contributions

[○]Q.C. and X.L. contributed equally to this work.

Notes

The authors declare no competing financial interest.

■ ACKNOWLEDGMENTS

Q.C. was supported by the China Scholarship Council (201908500058) and the National Natural Science Foundation of China (31901183). J.P.G. was supported by the Canada Research Chair program and a Distinguished Visiting Professorship in the Department of Environmental Sciences, Baylor University in Waco, TX, U.S.A.

■ REFERENCES

- (1) Wang, G.; Du, Z.; Chen, H.; Su, Y.; Gao, S.; Mao, L. Tissue-specific accumulation, depuration, and transformation of triphenyl phosphate (TPHP) in adult zebrafish (*Danio rerio*). *Environ. Sci. Technol.* **2016**, *50* (24), 13555–13564.
- (2) Ballesteros-Gómez, A.; Van den Eede, N.; Covaci, A. *In vitro* human metabolism of the flame retardant resorcinol bis-(diphenylphosphate) (RDP). *Environ. Sci. Technol.* **2015**, *49* (6), 3897–3904.
- (3) Shen, J.; Zhang, Y.; Yu, N.; Crump, D.; Li, J.; Su, H.; Letcher, R. J.; Su, G. Organophosphate ester, 2-ethylhexyl diphenyl phosphate (EHDP), elicits cytotoxic and transcriptomic effects in chicken embryonic hepatocytes and its biotransformation profile compared to humans. *Environ. Sci. Technol.* **2019**, *53* (4), 2151–2160.
- (4) Liu, Y.; Gong, S.; Ye, L.; Li, J.; Liu, C.; Chen, D.; Fang, M.; Letcher, R. J.; Su, G. Organophosphate (OP) diesters and a review of sources, chemical properties, environmental occurrence, adverse effects, and future directions. *Environ. Int.* **2021**, *155*, 106691.
- (5) Zhao, F.; Kang, Q.; Zhang, X.; Liu, J.; Hu, J. Urinary biomarkers for assessment of human exposure to monomeric aryl phosphate flame retardants. *Environ. Int.* **2019**, *124*, 259–264.
- (6) Jayatilaka, N. K.; Restrepo, P.; Davis, Z.; Vidal, M.; Calafat, A. M.; Ospina, M. Quantification of 16 urinary biomarkers of exposure to flame retardants, plasticizers, and organophosphate insecticides for biomonitoring studies. *Chemosphere* **2019**, *235*, 481–491.
- (7) Ospina, M.; Jayatilaka, N. K.; Wong, L.-Y.; Restrepo, P.; Calafat, A. M. Exposure to organophosphate flame retardant chemicals in the U.S. general population: Data from the 2013–2014 National Health and Nutrition Examination Survey. *Environ. Int.* **2018**, *110*, 32–41.
- (8) Butt, C. M.; Congleton, J.; Hoffman, K.; Fang, M.; Stapleton, H. M. Metabolites of organophosphate flame retardants and 2-ethylhexyl tetrabromobenzoate in urine from paired mothers and toddlers. *Environ. Sci. Technol.* **2014**, *48* (17), 10432–10438.
- (9) Björnsdotter, M. K.; Romera-García, E.; Borrull, J.; de Boer, J.; Rubio, S.; Ballesteros-Gómez, A. Presence of diphenyl phosphate and aryl-phosphate flame retardants in indoor dust from different microenvironments in Spain and the Netherlands and estimation of human exposure. *Environ. Int.* **2018**, *112*, 59–67.
- (10) Kim, U.-J.; Oh, J. K.; Kannan, K. Occurrence, removal, and environmental emission of organophosphate flame retardants/

plasticizers in a wastewater treatment plant in New York State. *Environ. Sci. Technol.* **2017**, *51* (14), 7872–7880.

(11) Funk, S. P.; Duffin, L.; He, Y.; McMullen, C.; Sun, C.; Utting, N.; Martin, J. W.; Goss, G. G.; Alessi, D. S. Assessment of impacts of diphenyl phosphate on groundwater and near-surface environments: sorption and toxicity. *J. Contam. Hydrol.* **2019**, *221*, 50–57.

(12) García-López, M.; Rodríguez, I.; Cela, R. Mixed-mode solid-phase extraction followed by liquid chromatography–tandem mass spectrometry for the determination of tri- and di-substituted organophosphorus species in water samples. *J. Chromatogr. A* **2010**, *1217* (9), 1476–1484.

(13) Wang, Y.; Kannan, P.; Halden, R. U.; Kannan, K. A nationwide survey of 31 organophosphate esters in sewage sludge from the United States. *Sci. Total Environ.* **2019**, *655*, 446–453.

(14) Li, Y.; Kang, Q.; Chen, R.; He, J.; Liu, L.; Wang, L.; Hu, J. 2-Ethylhexyl diphenyl phosphate and its hydroxylated metabolites are anti-androgenic and cause adverse reproductive outcomes in male Japanese Medaka (*Oryzias latipes*). *Environ. Sci. Technol.* **2020**, *54* (14), 8919–8925.

(15) Li, Y.; Ma, H.; Chen, R.; Zhang, H.; Nakanishi, T.; Hu, J. Maternal transfer of 2-ethylhexyl diphenyl phosphate leads to developmental toxicity possibly by blocking the retinoic acid receptor and retinoic X receptor in Japanese Medaka (*Oryzias latipes*). *Environ. Sci. Technol.* **2021**, *55* (8), 5056–5064.

(16) Luo, D.; Liu, W.; Tao, Y.; Wang, L.; Yu, M.; Hu, L.; Zhou, A.; Covaci, A.; Xia, W.; Li, Y.; Xu, S.; Mei, S. Prenatal exposure to organophosphate flame retardants and the risk of low birth weight: A nested case-control study in China. *Environ. Sci. Technol.* **2020**, *54* (6), 3375–3385.

(17) Preston, E. V.; McClean, M. D.; Claus Henn, B.; Stapleton, H. M.; Bravenman, L. E.; Pearce, E. N.; Makey, C. M.; Webster, T. F. Associations between urinary diphenyl phosphate and thyroid function. *Environ. Int.* **2017**, *101*, 158–164.

(18) Su, G.; Crump, D.; Letcher, R. J.; Kennedy, S. W. Rapid *in vitro* metabolism of the flame retardant triphenyl phosphate and effects on cytotoxicity and mRNA expression in chicken embryonic hepatocytes. *Environ. Sci. Technol.* **2014**, *48* (22), 13511–13519.

(19) Li, Y.; Yao, C.; Zheng, Q.; Yang, W.; Niu, X.; Zhang, Y.; Lu, G. Occurrence and ecological implications of organophosphate triesters and diester degradation products in wastewater, river water, and tap water. *Environ. Pollut.* **2020**, *259*, 113810.

(20) Zhang, Q.; Yu, C.; Fu, L.; Gu, S.; Wang, C. New insights in the endocrine disrupting effects of three primary metabolites of organophosphate flame retardants. *Environ. Sci. Technol.* **2020**, *54* (7), 4465–4474.

(21) Mitchell, C. A.; Reddam, A.; Dasgupta, S.; Zhang, S.; Stapleton, H. M.; Volz, D. C. Diphenyl phosphate-induced toxicity during embryonic development. *Environ. Sci. Technol.* **2019**, *53* (7), 3908–3916.

(22) Lee, J. S.; Morita, Y.; Kawai, Y. K.; Covaci, A.; Kubota, A. Developmental circulatory failure caused by metabolites of organophosphorus flame retardants in zebrafish, *Danio rerio*. *Chemosphere* **2020**, *246*, 125738.

(23) Selmi-Ruby, S.; Marín-Sáez, J.; Fildier, A.; Buleté, A.; Abdallah, M.; Garcia, J.; Deverchère, J.; Spinner, L.; Giroud, B.; Ibanez, S.; Granjon, T.; Bardel, C.; Puisieux, A.; Fervers, B.; Vulliet, E.; Payen, L.; Vigneron, A. M. *In vivo* characterization of the toxicological properties of DPhP, one of the main degradation products of aryl phosphate esters. *Environ. Health Perspect.* **2020**, *128* (12), 127006–127006.

(24) Rodil, R.; Quintana, J. B.; Concha-Graña, E.; López-Mahía, P.; Muniategui-Lorenzo, S.; Prada-Rodríguez, D. Emerging pollutants in sewage, surface and drinking water in Galicia (NW Spain). *Chemosphere* **2012**, *86* (10), 1040–1049.

(25) Liu, X.; Jung, D.; Jo, A.; Ji, K.; Moon, H.-B.; Choi, K. Long-term exposure to triphenylphosphate alters hormone balance and HPG, HPI, and HPT gene expression in zebrafish (*Danio rerio*). *Environ. Toxicol. Chem.* **2016**, *35* (9), 2288–2296.

(26) Krumm, E. A.; Patel, V. J.; Tillery, T. S.; Yasrebi, A.; Shen, J.; Guo, G. L.; Marco, S. M.; Buckley, B. T.; Roepke, T. A.

Organophosphate flame-retardants alter adult mouse homeostasis and gene expression in a sex-dependent manner potentially through interactions with ER α . *Toxicol. Sci.* **2018**, *162* (1), 212–224.

(27) Liu, X.; Cai, Y.; Wang, Y.; Xu, S.; Ji, K.; Choi, K. Effects of tris(1,3-dichloro-2-propyl) phosphate (TDCPP) and triphenyl phosphate (TPP) on sex-dependent alterations of thyroid hormones in adult zebrafish. *Ecotoxicol. Environ. Saf.* **2019**, *170*, 25–32.

(28) Zhang, Q.-F.; Li, Y.-W.; Liu, Z.-H.; Chen, Q.-L. Exposure to mercuric chloride induces developmental damage, oxidative stress and immunotoxicity in zebrafish embryos-larvae. *Aquat. Toxicol.* **2016**, *181*, 76–85.

(29) Rui, L. Energy metabolism in the liver. *Compr. Physiol.* **2014**, *4* (1), 177–197.

(30) Gong, Y.; Zhang, K.; Geng, N.; Wu, M.; Yi, X.; Liu, R.; Challis, J. K.; Codling, G.; Xu, E. G.; Giesy, J. P. Molecular mechanisms of zooplanktonic toxicity in the okadaic acid-producing dinoflagellate *Prorocentrum lima*. *Environ. Pollut.* **2021**, *279*, 116942.

(31) Zheng, F.; Zhao, X.; Zeng, Z.; Wang, L.; Lv, W.; Wang, Q.; Xu, G. Development of a plasma pseudotargeted metabolomics method based on ultra-high-performance liquid chromatography–mass spectrometry. *Nat. Protoc.* **2020**, *15* (8), 2519–2537.

(32) Xia, J.; Psychogios, N.; Young, N.; Wishart, D. S. MetaboAnalyst: a web server for metabolomic data analysis and interpretation. *Nucleic Acids Res.* **2009**, *37*, W652–W660.

(33) Barupal, D. K.; Fiehn, O. Chemical similarity enrichment analysis (ChemRICH) as alternative to biochemical pathway mapping for metabolomic datasets. *Sci. Rep.* **2017**, *7* (1), 14567.

(34) Contrepolis, K.; Wu, S.; Moneghetti, K. J.; Hornburg, D.; Ahadi, S.; Tsai, M.-S.; Metwally, A. A.; Wei, E.; Lee-McMullen, B.; Quijada, J. V.; Chen, S.; Christle, J. W.; Ellenberger, M.; Balliu, B.; Taylor, S.; Durrant, M. G.; Knowles, D. A.; Choudhry, H.; Ashland, M.; Bahmani, A.; Enslin, B.; Amsellem, M.; Kobayashi, Y.; Avina, M.; Perelman, D.; Schüssler-Fiorenza Rose, S. M.; Zhou, W.; Ashley, E. A.; Montgomery, S. B.; Chaib, H.; Haddad, F.; Snyder, M. P. Molecular choreography of acute exercise. *Cell* **2020**, *181* (5), 1112–1130. e16.

(35) Yu, G.; Wang, L. G.; Han, Y.; He, Q. Y. ClusterProfiler: an R package for comparing biological themes among gene clusters. *OMICS* **2012**, *16* (5), 284–7.

(36) Kolde, R. P. Heatmap: pretty heatmaps. R package version 1.0.12., **2021**; <http://CRAN.R-project.org/package=heatmap>. Date of Access: August 1, 2021.

(37) Su, G.; Letcher, R. J.; Yu, H. Organophosphate flame retardants and plasticizers in aqueous solution: pH-dependent hydrolysis, kinetics, and pathways. *Environ. Sci. Technol.* **2016**, *50* (15), 8103–8111.

(38) Ren, R.; Zhai, L.; Tian, Q.; Meng, D.; Guan, Z.; Cai, Y.; Liao, X. Identification of a novel glycerophosphodiester phosphodiesterase from *Bacillus altitudinis* W3 and its application in degradation of diphenyl phosphate. *3 Biotech* **2021**, *11* (4), 161.

(39) Li, Y.; Chen, R.; He, J.; Ma, H.; Zhao, F.; Tao, S.; Liu, J.; Hu, J. Triphenyl phosphate at environmental levels retarded ovary development and reduced egg production in Japanese Medaka (*Oryzias latipes*). *Environ. Sci. Technol.* **2019**, *53* (24), 14709–14715.

(40) Li, Y.; Wang, C.; Zhao, F.; Zhang, S.; Chen, R.; Hu, J. Environmentally relevant concentrations of the organophosphorus flame retardant triphenyl phosphate impaired testicular development and reproductive behaviors in Japanese Medaka (*Oryzias latipes*). *Environ. Sci. Technol. Lett.* **2018**, *5* (11), 649–654.

(41) Li, J.; Zhao, L.; Letcher, R. J.; Zhang, Y.; Jian, K.; Zhang, J.; Su, G. A review on organophosphate Ester (OPE) flame retardants and plasticizers in foodstuffs: Levels, distribution, human dietary exposure, and future directions. *Environ. Int.* **2019**, *127*, 35–51.

(42) Hollywood, K.; Brison, D. R.; Goodacre, R. Metabolomics: Current technologies and future trends. *Proteomics* **2006**, *6* (17), 4716–4723.

(43) Jordan, K. W.; Nordenstam, J.; Lauwers, G. Y.; Rothenberger, D. A.; Alavi, K.; Garwood, M.; Cheng, L. L. Metabolomic characterization of human rectal adenocarcinoma with intact tissue

magnetic resonance spectroscopy. *Dis. Colon Rectum* **2009**, *52* (3), 520.

(44) Tocher, D. R. Metabolism and functions of lipids and fatty acids in teleost fish. *Rev. Fish. Sci.* **2003**, *11* (2), 107–184.

(45) Pan, H.; Li, L.-Y.; Li, J.-M.; Wang, W.-L.; Limbu, S. M.; Degrace, P.; Li, D.-L.; Du, Z.-Y. Inhibited fatty acid β -oxidation impairs stress resistance ability in Nile tilapia (*Oreochromis niloticus*). *Fish Shellfish Immunol.* **2017**, *68*, 500–508.

(46) Wang, D.; Zhu, W.; Chen, L.; Yan, J.; Teng, M.; Zhou, Z. Neonatal triphenyl phosphate and its metabolite diphenyl phosphate exposure induce sex- and dose-dependent metabolic disruptions in adult mice. *Environ. Pollut.* **2018**, *237*, 10–17.

(47) Wang, D.; Yan, S.; Yan, J.; Teng, M.; Meng, Z.; Li, R.; Zhou, Z.; Zhu, W. Effects of triphenyl phosphate exposure during fetal development on obesity and metabolic dysfunctions in adult mice: Impaired lipid metabolism and intestinal dysbiosis. *Environ. Pollut.* **2019**, *246*, 630–638.

(48) Du, Z.; Zhang, Y.; Wang, G.; Peng, J.; Wang, Z.; Gao, S. TPHP exposure disturbs carbohydrate metabolism, lipid metabolism, and the DNA damage repair system in zebrafish liver. *Sci. Rep.* **2016**, *6* (1), 21827.

(49) Wang, L.; Huang, X.; Lim, D. J.; Laserna, A. K. C.; Li, S. F. Y. Uptake and toxic effects of triphenyl phosphate on freshwater microalgae *Chlorella vulgaris* and *Scenedesmus obliquus*: Insights from untargeted metabolomics. *Sci. Total Environ.* **2019**, *650*, 1239–1249.

(50) Wang, L.; Huang, X.; Laserna, A. K. C.; Li, S. F. Y. Untargeted metabolomics reveals transformation pathways and metabolic response of the earthworm *Perionyx excavatus* after exposure to triphenyl phosphate. *Sci. Rep.* **2018**, *8* (1), 16440.

(51) Subramanian, A.; Tamayo, P.; Mootha, V. K.; Mukherjee, S.; Ebert, B. L.; Gillette, M. A.; Paulovich, A.; Pomeroy, S. L.; Golub, T. R.; Lander, E. S.; Mesirov, J. P. Gene set enrichment analysis: a knowledge-based approach for interpreting genome-wide expression profiles. *Proc. Natl. Acad. Sci. U. S. A.* **2005**, *102* (43), 15545.

(52) Legradi, J.; Dahlberg, A.-K.; Cenijn, P.; Marsh, G.; Asplund, L.; Bergman, Å.; Legler, J. Disruption of oxidative phosphorylation (OXPHOS) by hydroxylated polybrominated diphenyl ethers (OH-PBDEs) present in the marine environment. *Environ. Sci. Technol.* **2014**, *48* (24), 14703–14711.

(53) Boxtel, A. L. v.; Kamstra, J. H.; Cenijn, P. H.; Pieterse, B.; Wagner, M. J.; Antink, M.; Krab, K.; Burg, B. v. d.; Marsh, G.; Brouwer, A.; Legler, J. Microarray analysis reveals a mechanism of phenolic polybrominated diphenylether toxicity in zebrafish. *Environ. Sci. Technol.* **2008**, *42* (5), 1773–1779.

(54) Wallace, K. B.; Starkov, A. A. Mitochondrial targets of drug toxicity. *Annu. Rev. Pharmacol. Toxicol.* **2000**, *40* (1), 353–388.

(55) Limbu, S. M.; Zhou, L.; Sun, S.-X.; Zhang, M.-L.; Du, Z.-Y. Chronic exposure to low environmental concentrations and legal aquaculture doses of antibiotics cause systemic adverse effects in Nile tilapia and provoke differential human health risk. *Environ. Int.* **2018**, *115*, 205–219.

(56) Ussery, E.; Bridges, K. N.; Pandelides, Z.; Kirkwood, A. E.; Bonetta, D.; Venables, B. J.; Guchardi, J.; Holdway, D. Effects of environmentally relevant metformin exposure on Japanese medaka (*Oryzias latipes*). *Aquat. Toxicol.* **2018**, *205*, 58–65.

(57) Zou, W.; Zhang, X.; Ouyang, S.; Hu, X.; Zhou, Q. Graphene oxide nanosheets mitigate the developmental toxicity of TDCIPP in zebrafish via activating the mitochondrial respiratory chain and energy metabolism. *Sci. Total Environ.* **2020**, *727*, 138486.

(58) Wakil, S. J.; Abu-Elheiga, L. A. Fatty acid metabolism: target for metabolic syndrome. *J. Lipid Res.* **2009**, *50*, S138–S143.

(59) McGarry, J. D.; Brown, N. F. The mitochondrial carnitine palmitoyltransferase system — from concept to molecular analysis. *Eur. J. Biochem.* **1997**, *244* (1), 1–14.

(60) Klein, J. Membrane breakdown in acute and chronic neurodegeneration: focus on choline-containing phospholipids. *J. Neural Transm.* **2000**, *107* (8), 1027–1063.

(61) Hollie, N. I.; Cash, J. G.; Matlib, M. A.; Wortman, M.; Basford, J. E.; Abplanalp, W.; Hui, D. Y. Micromolar changes in

lysophosphatidylcholine concentration cause minor effects on mitochondrial permeability but major alterations in function. *Biochim. Biophys. Acta, Mol. Cell Biol. Lipids* **2014**, *1841* (6), 888–895.

(62) Peters, R. H. The ecological implications of body size. *Cambridge studies in ecology* **1983**, 235–238.

(63) Dickerson, B. R.; Quinn, T. P.; Willson, M. F. Body size, arrival date, and reproductive success of pink salmon, *Oncorhynchus gorbuscha*. *Ethology Ecology & Evolution* **2002**, *14* (1), 29–44.

(64) Speakman, J. R. Body size, energy metabolism and lifespan. *J. Exp. Biol.* **2005**, *208* (9), 1717–1730.

(65) Steele, S. L.; Prykhodzij, S. V.; Berman, J. N. Zebrafish as a model system for mitochondrial biology and diseases. *Transl. Res.* **2014**, *163* (2), 79–98.

(66) Bambino, K.; Chu, J. Zebrafish in Toxicology and Environmental Health. In *Current Topics in Developmental Biology*; Sadler, K. C., Ed.; Academic Press: 2017; Vol. 124, pp 331–367.

1 *Supporting information for*

2 **Life Cycle Exposure to Environmentally Relevant Concentrations of**
3 **Diphenyl Phosphate (DPhP) Inhibits Growth and Energy Metabolism of**
4 **Zebrafish in a Sex-Specific Manner**

5

6 Qiliang Chen^{1,#}, Xiaolong Lian^{1,#}, Jingjing An¹, Ningbo Geng^{2,*}, Haijun Zhang², Jonathan
7 K. Challis³, Yun Luo², Yaxin Liu⁴, Guanyong Su⁴, Yuwei Xie³, Yingwen Li¹, Zhihao Liu¹,
8 Yanjun Shen¹, John P. Giesy^{3, 5, 6, 7}, Yufeng Gong^{3,*}

9

10 ¹ *Chongqing Key Laboratory of Animal Biology, School of Life Sciences, Chongqing*
11 *Normal University, Chongqing, China*

12 ² *CAS Key Laboratory of Separation Sciences for Analytical Chemistry, Dalian Institute of*
13 *Chemical Physics, Chinese Academy of Sciences, Dalian, China*

14 ³ *Toxicology Centre, University of Saskatchewan, Saskatoon, SK, Canada*

15 ⁴ *School of Environmental and Biological Engineering, Nanjing University of Science and*
16 *Technology, Nanjing, Jiangsu, China*

17 ⁵ *Department of Veterinary Biomedical Sciences, University of Saskatchewan, Saskatoon,*
18 *SK, Canada*

19 ⁶ *Department of Environmental Sciences, Baylor University, Waco, Texas, USA*

20 ⁷ *State Key Laboratory of Pollution Control and Resource Reuse, School of the*
21 *Environment, Nanjing University, Nanjing, China*

22

23 # These authors contributed equally to this work.

24 *Corresponding author

25 *E-mail addresses:* yufeng.gong@usask.ca (Dr. Yufeng Gong); gengningbo@dicp.ac.cn

26 (Dr. Ningbo Geng).

27

28 *Number of pages:* 28

29 *Number of tables:* 6

30 *Number of figures:* 6

31

32 **Contents:**

33 1. Zebrafish maintenance and exposure design

34 2. Quantification of DPhP in water

35 3. Sample preparation and instrumental analysis for pseudo-targeted metabolomics

36 4. RNA isolation and sequencing

37 5. Quantitative real time PCR (qRT-PCR)

38

39 **Tables**

40 **Table S1.** Summary statistics of transcriptome sequencing

41 **Table S2.** Annotation of zebrafish transcriptome

42 **Table S3.** Measured concentrations of DPhP in water

43 **Table S4.** Significantly enriched Wikipathways by gene set enrichment analysis (GSEA)

44 **Table S5.** Primer sequences used in qRT-PCR

45 **Table S6.** qRT-PCR validation of transcriptomic data

46

47 **Figures**

48 **Figure S1.** Stability test of DPhP

49 **Figure S2.** Effects of DPhP exposure on survival rate, condition factor, and hepatosomatic
50 index in zebrafish

51 **Figure S3.** Reproducibility of pseudo-targeted metabolomics analysis for pooled QC

52 **Figure S4.** Wikipathways enrichment analysis of female zebrafish using gene set
53 enrichment analysis (GSEA) algorithm

54 **Figure S5.** Expression levels of genes related to fatty acid oxidation in female zebrafish
55 liver

56 **Figure S6.** Up-regulated catabolism of PC molecules in male zebrafish liver after life cycle
57 exposure to DPhP at environmentally realistic concentrations

58

59 **1. Zebrafish maintenance and exposure design**

60 The current experiment was approved by the University of Saskatchewan (AUP#
61 20200065). Embryos were collected from healthy adult zebrafish (wildtype, AB strain)
62 according to [Zhang et al. \(2016\)](#)¹. Embryos that had developed normally and reached the
63 blastula stage (2 h post fertilization, hpf) were randomly distributed into 16 tanks (length
64 20 cm, width 14 cm, height 8 cm) containing 1 L exposure solution with nominal
65 concentrations of DPhP at 0, 1, 10, or 100 µg/L, with 150 embryos per tank and 4 replicate
66 tanks for each treatment. Exposure tanks were placed in an incubator (14h/10h day/night
67 cycle, 28 °C) for 20 days for embryo hatching and larval culture. At 21 days post
68 fertilization (dpf), the fish in the incubator were transferred to a semi-static system
69 (14h/10h day/night cycle, 28 °C) and continued to be exposed to DPhP until 120 dpf (also
70 four replicated tanks for each concentration). During the exposure, residual food and feces
71 in tanks were removed every day, and half of the water in each tank was replaced every 2
72 days with fresh aerated tap water containing the desired concentration of DPhP. During the
73 experimental period, fish were transferred to larger tanks as they grew to ensure that the
74 experimental fish had enough living space, and the number of fish in each tank remained
75 approximately equal, with a density of about 120, 60, 10, and 5 fish per liter of water during
76 the periods of 6–15 dpf, 16–30 dpf, 31–60 dpf, and 61–120 dpf, respectively. Fish were fed
77 to apparent satiation thrice daily with live *Paramecia*, live *Paramecia* and *Artemia*, and
78 live *Artemia* and commercial pellet diet during periods of 6–20 dpf, 21–50 dpf, and 51–
79 120 dpf, respectively. Water quality conditions were monitored and were: temperature,
80 27±0.3 °C; pH, 7.7±0.1; dissolved oxygen> 6 mg/L. After a 120-day exposure, all fish were
81 anesthetized with 0.01% MS-222 and dissected humanely after measurement of body

82 length and body mass. Livers were excised and weighted to calculate the hepatosomatic
83 index (HSI), determined as [liver mass (g)/body mass (g) × 100%]. Then, all liver samples
84 were flash-frozen in liquid nitrogen and stored at −80 °C for the analysis of metabolomics,
85 transcriptomics, and enzyme activity. The sex of the fish was determined by visual
86 inspection of gonadal morphology. The average sex ratio (proportion males) was 59.7%.
87

88 **2. Quantification of DPhP in water**

89 The exposure solutions from each treatment group were first centrifuged at 14,000 g for
90 10 mins. Then, the supernatant was collected and mixed with LC-MS grade methanol at a
91 ratio of 9: 1. A Waters Acquity Ultra Performance liquid chromatography system (UPLC)
92 coupled online with an ABI Q-Trap 5500 (AB SCIEX, USA) via an electrospray ionization
93 (ESI) interface was used for DPhP analysis. Chromatographic separation was carried out
94 with an ACQUITY UPLC HSS T3 column (2.1 mm × 100 mm × 1.8 μm, Waters, USA)
95 maintained at 40 °C. Mobile phase A consisted of 0.1% formic acid in water; mobile phase
96 B was LC-MS grade acetonitrile. The flow rate was set at 0.30 mL/min. Injection volume
97 was set at 5 μL. The elution gradient was performed as follows: 0–8 min, 20–100% B; 8–
98 8.5 min, 100–20% B; 8.5–10 min, 20% B for column equilibration. The ESI source was set
99 with the following parameters: ion source, turbo spray; source temperature 500 °C; ion
100 spray voltage (IS) –4500 V. The ion source gas I (GSI), gas II (GSII), and curtain gas (CUR)
101 were set at 50, 50, and 25 psi, respectively; the collision gas (CAD) was medium. Multiple
102 reaction monitoring (MRM) experiments were carried out in negative ion mode by
103 selecting the following transitions (precursor ion > fragment ion): m/z 249.0 > 92.9, CE:
104 –35 and m/z 249.0 > 154.5, CE: –30. For the absolute quantification, external calibration
105 curves were prepared by injecting authentic standards of DPhP at different concentrations.
106

107 **3. Sample preparation and instrumental analysis for pseudo-targeted metabolomics**

108 Sample preparation

109 For pseudo-targeted metabolomics analysis, eight zebrafish livers of the same sex
110 randomly selected from the same exposure tank were pooled as one sample, and each
111 treatment group had eight pooled samples. There were two pooled samples for each
112 replicate tank and four replicate tanks for each treatment. Sample was mixed with 1 mL of
113 ultrapure water, homogenized, and then ultrasonically disrupted for 5 min in an ice-water
114 bath. The sample were subsequently freeze-dried and extracted with a mixture of
115 methanol/water (4: 1, v: v). Soon afterwards, the solution was vortexed for 30 min, and
116 then centrifuged for 20 min at $13,000 \times g$ and $4\text{ }^{\circ}\text{C}$. Finally, the supernatant was filtered by
117 an organic phase filter and transferred to a vial for metabolite analysis. Prior to extraction,
118 six kinds of internal standards (i.e., L-phenylalanine-d₅, octanoyl (8,8,8-d₃)-L-carnitine,
119 1-lauroyl-2-hydroxy-sn-glycero-3- phosphocholine, 1,2-diheptadecanoyl-sn-glycero-3-
120 phosphoethanolamine, hendecanoic acid, and nonadecanoic acid) were spiked into the
121 sample for the purpose of quality control.

122

123 UHPLC/Q-TOF MS for Untargeted Tandem MS

124 For untargeted tandem MS, the “auto MS/MS” function of the Q-TOF MS system with
125 data-dependent acquisition was performed in positive ion mode and negative ion mode,
126 respectively. For positive ion mode, 5 μL of extract containing metabolites was injected
127 into the UHPLC/Q-TOF MS system with an ACQUITY UPLC BEH C8 column (2.1 mm
128 \times 100 mm \times 1.7 μm , Waters, USA) maintained at $50\text{ }^{\circ}\text{C}$. Water and acetonitrile both
129 containing 0.1% (v/v) formic acid were used as mobile phases A and B, respectively. The

130 flow rate was 0.35 mL/min, and the gradient elution was as follows (time, %B): 0 min,
131 10%; 3 min, 40%; 15 min, 100%, and maintained for 5 min; 20.1 min, 10%, and re-
132 equilibrated for 2.9 min. The mass spectrometer was operated with a capillary voltage of
133 4000 V, fragmentor voltage of 175 V, skimmer voltage of 65 V, nebulizer gas (N₂) pressure
134 at 45 psi, drying gas (N₂) flow rate of 9 L/min, and a temperature of 350 °C. Five most
135 intense precursors were chosen within one full scan cycle (0.25 s) with a precursor ion scan
136 range of m/z 100–1000 and a tandem mass scan range of m/z 40–1000. The collision
137 energies were set at 10, 20, 30, and 40 eV, and all samples were analyzed to obtain abundant
138 and complementary product ion information.

139 For negative ion mode, 5 µL of extract containing metabolites was injected into the
140 UHPLC/Q-TOF MS system with an ACQUITY UPLC HSS T3 column (2.1 mm × 100
141 mm × 1.8 µm, Waters, USA) maintained at 50 °C. Water and methanol both containing 5
142 mmol/L ammonium bicarbonate were used as mobile phases A and B, respectively. The
143 flow rate was also 0.35 mL/min, and the gradient elution was as follows (time, %B): 0 min,
144 2%; 3 min, 42%; 12 min, 100%, and maintained for 4 min; 16.1 min, 2%, and re-
145 equilibrated for 3.9 min. The mass spectrometer was operated with a capillary voltage of
146 3500 V, fragmentor voltage of 175 V, skimmer voltage of 65 V, nebulizer gas (N₂) pressure
147 at 45 psi, drying gas (N₂) flow rate of 9 L/min, and a temperature of 350 °C. Five most
148 intense precursors were chosen within one full scan cycle (0.25 s) with a precursor ion scan
149 range of m/z 100–1000 and a tandem mass scan range of m/z 40–1000. The collision
150 energies were set at –10, –20, –30, and –40 eV, and all samples were analyzed to obtain
151 abundant and complementary product ion information.

152 After data acquisition, the “Find by Auto MS/MS” function of MassHunter Qualitative
153 Analysis software was used to automatically extract ion pair information for subsequent
154 MRM detection. The retention time window was set to 0.15 min; the MS/MS threshold
155 was set to 100, and the mass match tolerance was set to 0.02 Da. The single mass expansion
156 was set to symmetric 100 ppm, and the persistent background ions, such as reference mass
157 ions, were excluded. After execution, detected ion pairs with information about the
158 precursor ion, product ions, retention time, and collision energy were exported to a
159 spreadsheet. Ion pairs were selected on the basis of the following rules: different precursor
160 ions eluted in the neighboring time range were scrutinized to exclude the isotopic,
161 fragmentation, adduct, and dimer ions; and the product ion that appeared with the most
162 applied collision energy and with the highest intensity was selected as the characteristic
163 product ion.

164

165 UHPLC/Q-Trap MRM MS for Pseudo-targeted Metabolomic Analysis

166 A Waters Acquity Ultra Performance liquid chromatography system (UHPLC) coupled
167 online to an ABI Q-Trap 5500 (AB SCIEX, USA) via an electrospray ionization (ESI)
168 interface was adopted for pseudo-targeted metabolomics analysis using the spreadsheet
169 produced from the analysis of UHPLC/Q-TOF MS. The same chromatographic condition,
170 including chromatographic column, mobile phases, and gradient elution procedure, was
171 performed on both UHPLC/Q-TOF MS system and UHPLC/Q-Trap MS system.

172 For positive ion mode, The MS instrumental parameters were set as those for the
173 following: source temperature, 550 °C; gas I, 40 arbitrary units; gas II, 40 arbitrary units;
174 curtain gas, 35 arbitrary units; ion spray voltage, 5500 V.

175 For negative ion mode, The MS instrumental parameters were set as follows: source
176 temperature, 550 °C; gas I, 40 arbitrary units; gas II, 40 arbitrary units; curtain gas, 35
177 arbitrary units; ion spray voltage, -4500 V.

178

179 **4. RNA isolation and sequencing**

180 Livers of zebrafish exposed to nominal 0, 10, or 100 µg/L of DPhP were used for
181 transcriptomics. Each treatment group had three pooled samples and each pooled sample
182 had eight zebrafish livers of the same sex. Total RNA was isolated by TRIzol® reagent
183 (Invitrogen). RNA integrity and quality was determined with 1.5% agarose–formaldehyde
184 gel and an Agilent 2100 bioanalyzer (Agilent Technologies). RNA concentration were
185 measured by a NanoDrop spectrophotometer (Thermo Scientific) and only samples with a
186 260/280 nm ratio of 1.8–2.0 were analyzed further. The cDNA library was constructed with
187 Truseq™ RNA sample prep Kit (Illumina), and then next-generation sequencing was
188 performed on an Illumina HiSeq platform.

189 Raw data was processed by Cutadapt software (v1.16) and reads that contained adaptor
190 contamination, low quality bases, and undetermined bases were removed. Then, HISAT2
191 (v2.1.0) was used to map clean reads to the zebrafish genome (GRCz 11) and the mapped
192 reads of each sample were assembled using StringTie. Afterwards, assembled genes were
193 annotated for function against several public databases, including NCBI non-redundant
194 protein sequences (NR) database, Gene Ontology (GO) database, Kyoto Encyclopedia of
195 Genes and Genome (KEGG) database, Swiss-Prot database, Pfam database, and STRING
196 database. Transcript abundances were measured as Fragments per kilobase of transcript
197 sequence per millions base pairs sequenced (FPKM). Gene set enrichment analysis (GSEA)
198 was performed using Wikipathways database by R package clusterProfiler² to identify
199 pathways disrupted by DPhP. Transcriptomics data were validated through quantitative
200 real time PCR (qRT-PCR). Housekeeping elongation factor 1-alpha (*ef1a*) and ribosomal
201 protein L13a (*rpl13a*) were employed as reference genes.

202 **5. Quantitative real time PCR (qRT-PCR)**

203 Seven genes were randomly selected for validation of transcriptomics data by using
204 qRT-PCR. Primer sequences were listed in [Table S5](#). Sequences of these selected genes
205 were compared with the homologues (blastx) to verify our annotation. RNA samples of
206 zebrafish liver were extracted with the same method as described in transcriptomics
207 analysis, and concentrations of RNA were determined with Nano-100 (ALLSHENG,
208 Hangzhou, China). One microgram of isolated RNA was applied for complimentary DNA
209 (cDNA) synthesis with a PrimeScript™ RT reagent Kit (TaKaRa, Dalian, China). The
210 qRT-PCR were carried out on the CFX96™ Real-Time systems (Bio-Rad Laboratories,
211 USA) with a SYBR™ Premix Ex Taq™ reagent Kit (TaKaRa, Dalian, China) , and 1 μL
212 of cDNA templates were applied in each reaction. Elongation factor 1-alpha (*eflα*) and
213 ribosomal protein L13a (*rpl13a*) were adopted as the reference gene. Reaction conditions
214 were: 95 °C/ 30 s, 40 cycles of 95 °C/5 s, 60 °C/30 s and 72 °C/30 s. Melting curves were
215 determined with: 5 °C/1 min, and 80 cycles of 65 °C/5 s with 0.5 °C increase per cycle.
216 Relative expression of the target genes was calculated by $2^{-\Delta\Delta C_t}$ method.³

217

218 **Table S1.** Summary statistics of transcriptome sequencing

Sample	Raw reads	Clean reads	Error rate (%)	Q20 (%)	Q30 (%)	GC content (%)	rRNA ratio (%)
ML_Control_1	51817100	51720972	0.0278	96.77	91.79	46.15	7.22
ML_Control_2	50594170	50521064	0.0274	96.91	92.1	45.11	4.66
ML_Control_3	51993570	51864274	0.0276	96.85	91.94	46.52	4.43
ML_3.9 µg/L_1	47778272	47694118	0.0278	96.79	91.8	46.82	3.66
ML_3.9 µg/L_2	46791000	46732386	0.0269	97.15	92.53	46.81	3.84
ML_3.9 µg/L_3	50428250	50335198	0.0275	96.87	92.01	47.15	4.09
ML_35.6 µg/L_1	50854186	50678718	0.027	97.07	92.41	46.99	3.73
ML_35.6 µg/L_2	51442734	51269136	0.027	97.1	92.48	47.09	3.84
ML_35.6 µg/L_3	61094276	61056564	0.0249	98.04	94.32	46.58	4.33
FL_Control_1	43736490	43593800	0.0267	97.23	92.7	47.27	2.98
FL_Control_2	49600530	49454478	0.0265	97.32	92.92	47.26	3.12
FL_Control_3	39633198	39606716	0.0247	98.12	94.46	46.98	3.2
FL_3.9 µg/L_1	41825328	41725670	0.0297	96	90.31	47.03	3.01
FL_3.9 µg/L_2	46823970	46741222	0.0266	97.25	92.74	47.14	2.69
FL_3.9 µg/L_3	37464204	37446728	0.0256	97.78	93.59	46.73	2.8
FL_35.6 µg/L_1	50303526	50212844	0.0266	97.27	92.8	47.04	2.93
FL_35.6 µg/L_2	51158440	51044314	0.0267	97.25	92.71	47.22	2.82
FL_35.6 µg/L_3	40487274	40454702	0.0252	97.92	93.99	47.09	3.43

219 ML: male liver; FL: female liver.

220 **Table S2.** Annotation of zebrafish transcriptome

Databases	Number of annotated genes
NR	26633
GO	20769
KEGG	12794
Swiss-Prot	21305
Pfam	22731
STRING	14667

221

222 **Table S3.** Measured concentrations of DPhP in water

Sampling Date ^a	Measured DPhP concentrations in each exposure group (µg/L)			
	Control	1 µg/L DPhP	10 µg/L DPhP	100 µg/L DPhP
Day 83	< LOD ^b	0.7 ± 0.2	4.0 ± 1.0	32.8 ± 0.9
Day 97	< LOD	0.7 ± 0.3	4.1 ± 1.2	37.1 ± 15.9
Day 113	< LOD	1.0 ± 0.01	3.5 ± 0.6	36.8 ± 9.0
Average	< LOD	0.8 ± 0.2	3.9 ± 1.0	35.6 ± 9.9

223 **a.** Water samples were collected on day 83, 97, and 113 from the beginning of the exposure experiment and stored at -80 °C until analysis.

224 **b.** LOD: limit of detection.

225

226 **Table S4.** Significantly enriched Wikipathways by gene set enrichment analysis (GSEA)^a

ID	Description	Set size	NES ^b	P value	P adjusted
<i>Male, 3.9 µg/L DPhP treatment vs Control</i>					
WP1335	Oxidative phosphorylation	48	-2.28088	0.000254	0.006907
WP1339	Electron Transport Chain	85	-2.68924	0.000303	0.006907
WP467	mRNA processing	109	-1.90359	0.000334	0.006907
WP19	TCA Cycle	24	-1.77805	0.001504	0.023308
<i>Male, 35.6 µg/L DPhP treatment vs Control</i>					
WP1339	Electron Transport Chain	85	-2.02538	0.000124	0.007809
WP1335	Oxidative phosphorylation	47	-1.90715	0.002851	0.071938
WP1386	Integrin-mediated cell adhesion	34	1.850446	0.0042	0.071938
WP1356	Glycolysis and Gluconeogenesis	30	-1.85534	0.004568	0.071938
WP19	TCA Cycle	24	-1.76739	0.007609	0.095874
<i>Female, 3.9 µg/L DPhP treatment vs Control</i>					
WP152	FGF signaling pathway	52	-1.89411	0.000916	0.034337

WP402	ERK1 - ERK2 MAPK cascade	66	-1.78236	0.001232	0.034337
WP324	Cytoplasmic Ribosomal Proteins	77	-2.19789	0.001585	0.034337
WP1372	Oxidative Stress	23	-1.77673	0.00411	0.06679
WP1367	Transformation Growth Factor (TGF) beta Receptor Signaling Pathway	86	-1.53632	0.005871	0.076321

Female, 35.6 µg/L DPhP treatment vs Control

WP562	Exercise-induced Circadian Regulation	38	-2.06476	0.000173	0.007133
WP1387	Cholesterol Biosynthesis	13	2.141551	0.000223	0.007133
WP1339	Electron Transport Chain	85	1.78185	0.001599	0.034106
WP1335	Oxidative phosphorylation	47	1.780867	0.003223	0.051562
WP152	FGF signaling pathway	50	-1.69154	0.007155	0.091584
WP1337	MAPK Signaling Pathway	86	-1.57019	0.009712	0.103593

227 a. GSEA was performed with pre-ranked gene list by R package clusterProfiler. *P* adjusted < 0.1 was considered significant.

228 b. NES: normalized enrichment score.

229

230 **Table S5.** Primer sequences used in qRT-PCR

Gene symbol	NR database annotation	Primer sequences (5' → 3')
<i>ef1a</i>	Elongation factor 1-alpha	F: GATCACTGGTACTTCTCAGGCTGA R: GGTGAAAGCCAGGAGGGC
<i>rpl13a</i>	Ribosomal protein L13a	F: CCCGCGTGTCTTTCTTTTCC R: CTTGCTTGGCCACAATAGCG
<i>ndufb4</i>	NADH: ubiquinone oxidoreductase subunit B4	F: GAAGACCCTGCCCTTACCAG R: GGAATCCCTTTTGTCCCTGTCT
<i>cpt1b</i>	Carnitine palmitoyltransferase 1B	F: TGGCACTGCAACTAGCTCAA R: ACCTCTGCTCATTCGTGGTT
<i>cpt1ab</i>	Carnitine palmitoyltransferase 1Ab	F: TATGACGGACGCCTGTTGTT R: TTTGGCCCAGGGA ACTCTGT
<i>pdk2b</i>	Pyruvate dehydrogenase kinase 2b	F: TCCATTGCCTTTGTCAATGAAGC R: CATCAGACTTTGGACAAACCAGC
<i>acsl4a</i>	Acyl-CoA synthetase long chain family member 4a	F: GGC ACTATCACCGAAGTTGC R: CACATTAGGGCCACCGATGA
<i>per1b</i>	Period circadian clock 1b	F: CCAGGCAACGCTAAAGGTCC R: TGGGATGTGACAGAGGCAAC
<i>nrdl2b</i>	Nuclear receptor subfamily 1, group D, member 2b	F: AACGGTCTGGTGTCTGCTATG R: GCTCCTCCTGAAGAAACCCTTA

231

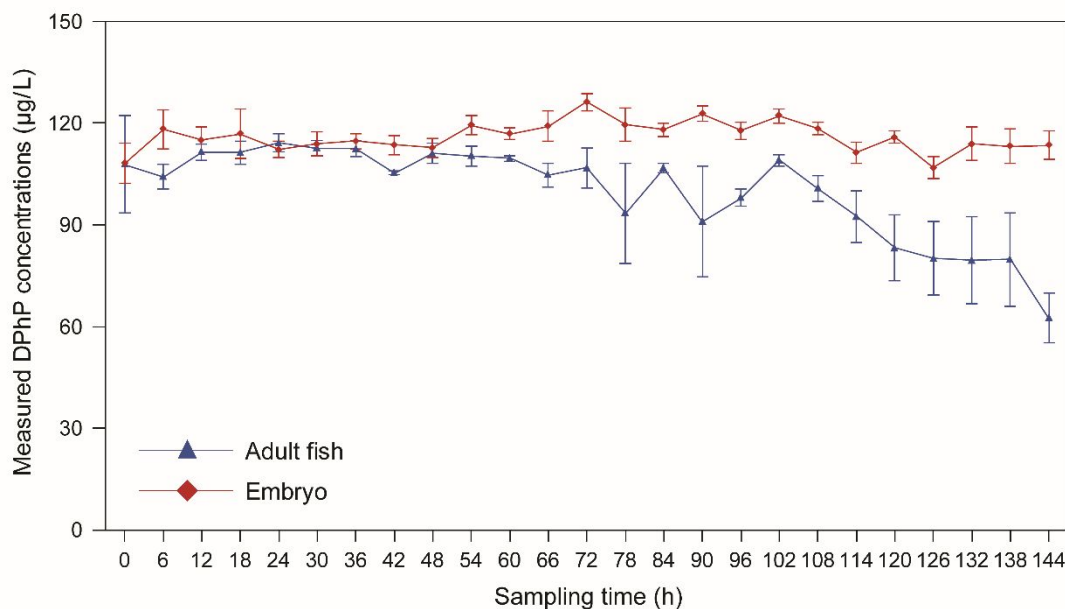
232 **Table S6.** qRT-PCR validation of transcriptomics data

Sex	Gene symbol	Ensembl ID	Measured conc. (µg/L)	DPhP	RNAseq		qRT-PCR		
					<i>P</i> value	Fold change	<i>P</i> value	Fold change ^a	
Male	<i>ndufb4</i>	ENSDARG00000019332	3.9		<u>0.003</u>	<u>0.430</u>	<u>0.020</u>	<u>0.744</u>	
			35.6		<u>0.039</u>	<u>0.554</u>	<u>0.005</u>	<u>0.743</u>	
	<i>cpt1b</i>	ENSDARG00000058285	3.9		0.088	0.613	0.161	0.698	
			35.6		<u>0.001</u>	<u>0.459</u>	<u>0.019</u>	<u>0.544</u>	
	<i>cpt1ab</i>	ENSDARG00000062054	3.9		0.175	0.700	0.276	0.798	
			35.6		<u>0.000</u>	<u>0.404</u>	<u>0.028</u>	<u>0.527</u>	
	<i>pdk2b</i>	ENSDARG00000059054	3.9		0.417	0.728	0.077	0.700	
			35.6		<u>0.000</u>	<u>0.104</u>	<u>0.000</u>	<u>0.253</u>	
	<i>acsl4a</i>	ENSDARG00000004078	3.9		0.778	0.917	0.658	0.861	
			35.6		<u>0.000</u>	<u>0.352</u>	<u>0.037</u>	<u>0.376</u>	
	Female	<i>nr1d2b</i>	ENSDARG00000009594	3.9		<u>0.001</u>	<u>0.256</u>	<u>0.000</u>	<u>0.475</u>
				35.6		<u>0.000</u>	<u>0.257</u>	<u>0.000</u>	<u>0.500</u>
<i>per1b</i>		ENSDARG00000012499	3.9		<u>0.000</u>	<u>0.082</u>	<u>0.013</u>	<u>0.525</u>	

		35.6	<u>0.000</u>	<u>0.101</u>	<u>0.004</u>	<u>0.463</u>
<i>cpt1ab</i>	ENSDARG00000062054	3.9	0.423	0.723	0.920	0.984
		35.6	0.271	0.710	0.869	0.972
<i>pdk2b</i>	ENSDARG00000059054	3.9	0.731	0.585	0.163	0.626
		35.6	<u>0.000</u>	<u>0.295</u>	<u>0.014</u>	<u>0.422</u>
<i>acsl4a</i>	ENSDARG00000004078	3.9	0.460	0.727	0.622	1.162
		35.6	0.672	1.082	0.320	1.387

233 a. Fold change was calculated as the ratio of the changes between DPhP treatment groups and the control group. Values with significant changes were
 234 highlighted (bold and underline).

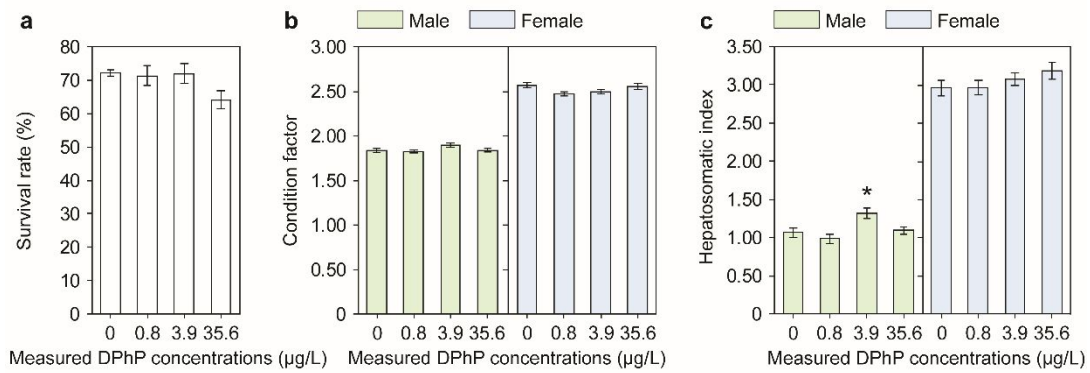
235



237

238 **Figure S1.** Stability test of DPhP. Zebrafish embryos or adults were exposed to nominal
 239 100 µg DPhP/L for 7 days. Water aliquots were sampled every 6 hours for DPhP
 240 measurement by UPLC-MS. There were three replicate tanks for each treatment and the
 241 exposure water were refreshed every 48 hours. In the exposure for embryos, there were
 242 150 zebrafish embryos (2 hpf) in 1 L water in each replicate tank (20 cm × 14 cm × 8 cm).
 243 In the exposure for zebrafish adults, there were 20 fish in 4 L water (2 g body mass/L) in
 244 each replicate tank (28 cm × 200 cm × 22 cm). Adult zebrafish were fed three times a day
 245 whereas zebrafish embryos were not fed during the test.

246

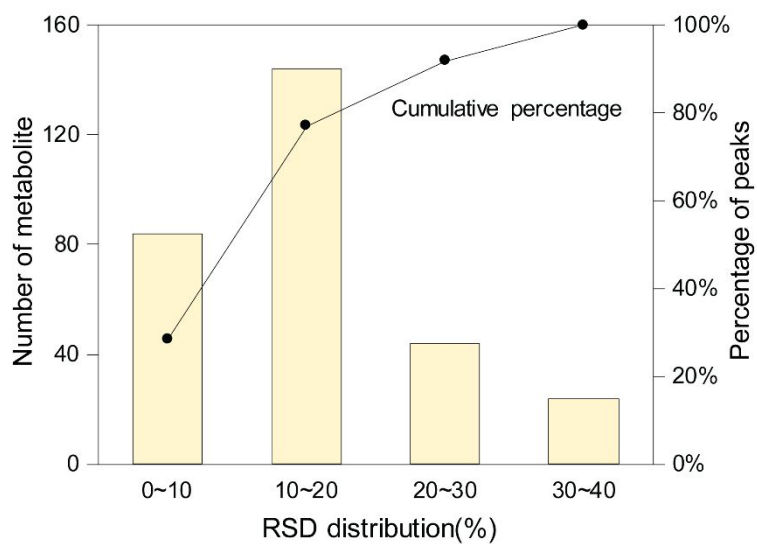


248

249 **Figure S2.** Effects of DPhP exposure on survival rate ($N = 4$ replicate tanks per treatment),
 250 condition factor ($N = 120$ fish per treatment), and hepatosomatic index ($N = 40$ fish per
 251 treatment) in zebrafish. The results are shown as the mean \pm SE. The asterisk indicates
 252 significant differences between DPhP treatments and control ($*0.01 < P < 0.05$).

253

254

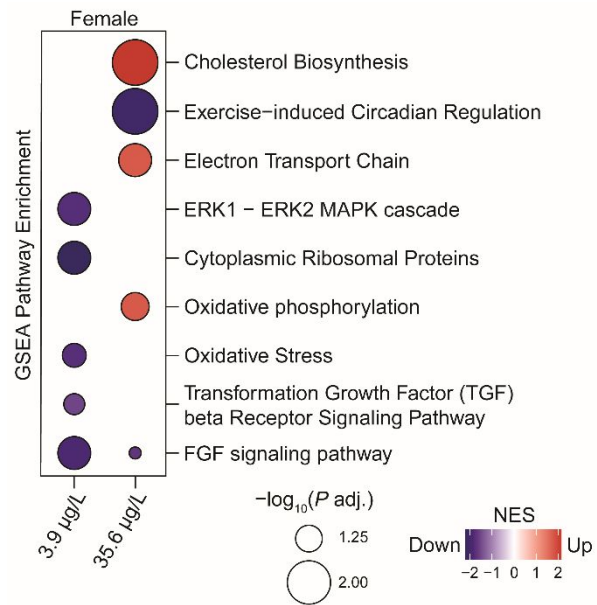


255

256 **Figure S3.** Reproducibility of pseudo-targeted metabolomics analysis for pooled QC. RSD:

257 relative standard deviation.

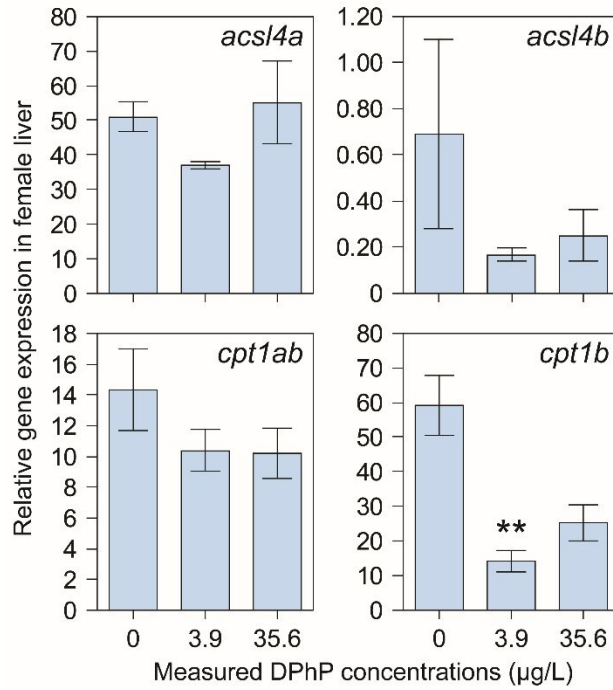
258



260

261 **Figure S4.** Wikipathways enrichment analysis of **female** zebrafish using gene set
 262 enrichment analysis (GSEA) algorithm. The dot size indicates pathway significance. The
 263 pathway direction is the normalized enrichment score (NES). Enriched pathways with P
 264 adjusted < 0.1 were considered significant.

265

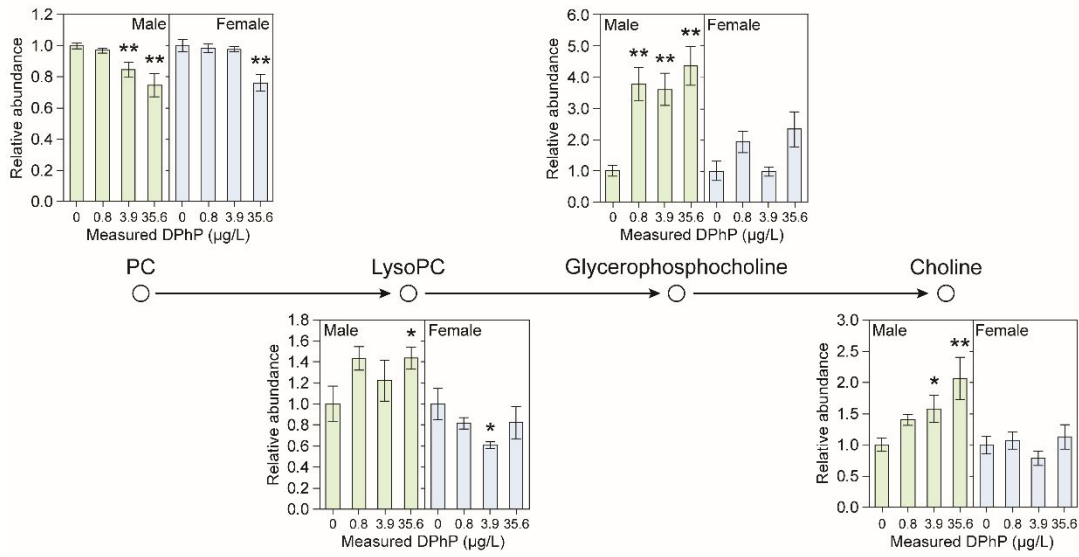


266

267 **Figure S5.** Expression levels of genes related to fatty acid oxidation in **female** zebrafish
 268 liver. *acsl4a*: acyl-CoA synthetase long-chain family member 4a; *acsl4b*: acyl-CoA
 269 synthetase long chain family member 4b; *cpt1ab*: carnitine palmitoyltransferase 1Ab;
 270 *cpt1b*: carnitine palmitoyltransferase 1B. Data are presented as mean \pm standard error (SE).
 271 *P* values are corrected by Bonferroni's method for multiple testing. The asterisk indicates
 272 significant differences between DPHP treatments and control (***P* < 0.01). *N* = 3.

273

274



275

276 **Figure S6.** Up-regulated catabolism of PC molecules in male zebrafish liver after life cycle

277 exposure to DPhP at environmentally realistic concentrations. PC: Phosphatidylcholine;

278 LysoPC: lysophosphatidylcholine. * $0.01 < P < 0.05$, ** $P < 0.01$. $N = 8$.

279

280 **References**

281 (1) Zhang, Q.-F.; Li, Y.-W.; Liu, Z.-H.; Chen, Q.-L., Exposure to mercuric chloride
282 induces developmental damage, oxidative stress and immunotoxicity in zebrafish embryos-
283 larvae. *Aquat. Toxicol.* **2016**, *181*, 76–85.

284 (2) Yu, G. C.; Wang, L. G.; Han, Y. Y.; He, Q. Y., ClusterProfiler: an R package for
285 comparing biological themes among gene clusters. *OMICS* **2012**, *16*, (5), 284–287.

286 (3) Livak, K. J.; Schmittgen, T. D., Analysis of relative gene expression data using
287 real-time quantitative PCR and the $2^{-\Delta\Delta CT}$ Method. *Methods* **2001**, *25*, (4), 402–408.

288